AALTO UNIVERSITY

School of Engineering

Department of Civil and Structural Engineering

Emma Skantz

Effect of elevated temperature on cement paste ageing

Master's thesis submitted in partial fulfilment of the requirements for the degree of Master of Science in Technology

Espoo, March 27, 2014

Supervisor: Prof. Jari Puttonen, Aalto University

Instructor: Lic. Sc. (Tech) Olli-Pekka Kari, Aalto University

Aalto University
School of Engineering

Aalto University, P.O. Box 12100, FI-00076 AALTO
www.aalto.fi

Abstract of master's thesis

Author	Emma Skantz
Title of thesis	Effect of elevated temperature on cement paste ageing
Department	Department of Civil and Structural Engineering
Professorship	Structural Engineering
Code of professorship	Rak-43
Thesis supervisor	Prof. Jari Puttonen
Thesis advisor(s) / Thesis examiner(s)	Lic. Sc. (Tech) Olli-Pekka Kari
Date	27.03.2014
Number of pages	72 +appendix 7
Language	English

Abstract

Long-term effects of elevated temperatures (65 °C - 345 °C) on the ageing of concrete and cement paste were studied. According to the literature review, harmful effects on ageing are porosity increase resulting from drying and dehydration of cement minerals, movement of moisture due to the uneven temperature, drying shrinkage, spalling, and carbonation. Delayed ettringite formation was found not to be significant when the exposure of cement paste or concrete to elevated temperatures lasts more than 2 days and there is no water storage after the exposure.

The laboratory tests were carried out for studying the effects of elevated temperatures on cement paste. The cement paste specimens made of ordinary or sulphate resisting portland cement were exposed to temperatures of 95 °C, 175 °C and 345 °C for 124 days and also to cooling cycles in water and relative humidity 45%. The specimens were studied with thermal analysis and x-ray diffraction. Compressive strength and porosity tests were also performed. Decreasing of portlandite and increasing of calcite was observed when the exposure temperature was risen. Porosity increased as the exposure temperature increased and compression strength after 124 days in 345 °C was 70-80% of original. Ordinary portland cement behaved better than sulphate resistant cement at elevated temperatures, in respect of porosity and compressive strength.

In the study, the ageing was also simulated numerically. The numerical model was implemented in geochemical Crunchflow software. The simulations were compared to the values received from laboratory experiments and the same agreements were observed but also clear deviations indicating needs for further research. The simulations were performed for predicting the phenomena after one and two years of exposure. Simulations showed that even after 124 d in 175 °C not all calcium-silicate-hydrate has disappeared, it did decompose after two years of exposure. According to the calculations at the temperature of 345 °C almost all cement hydrates are decomposed and only dicalciumsilicate is left.

Calculations and experimental results suggest that temperature of 95 °C cannot be considered detrimental for cement paste. Temperature of 175 °C is not harmful for short periods, but after 1 year, almost all C-S-H is decomposed. 345 °C is harmful for cement paste also for short periods. In the simulations no differences were observed between the behaviour of different cements at the elevated temperatures.

Keywords cement paste, elevated temperature, simulation

Aalto University
School of Engineering

Aalto University, P.O. Box 12100, FI-00076 AALTO
www.aalto.fi

Abstract of master's thesis

Tekijä Emma Skantz

Työn nimi Kohonneen lämpötilan vaikutukset sementtipastan vanhenemiselle

Laitos Rakenne- ja rakennustuotantotekniikka

Professuuri Talonrakennustekniikka **Professuurikoodi** Rak-43

Työn valvoja Prof. Jari Puttonen

Työn ohjaaja(t)/Työn tarkastaja(t) TkL Olli-Pekka Kari

Päivämäärä 27.03.2014 **Sivumäärä** 72 + liitteet 7 **Kieli** englanti

Tiivistelmä

Työssä tutkittiin kohonneen lämpötilan (65 °C - 345 °C) vaikutuksia betoniin ja sementtipastaan. Kohonneesta lämpötilasta aiheutuva huokoisuuden kasvaminen dehydrataation ja kuivumisen takia, epätasaisesta lämpötilasta johtuva kosteuden siirtyminen, kuivumiskutistuminen, hajoaminen ja karbonatisoituminen ovat kirjallisuustutkimuksen mukaan haitallisia vaikutuksia betonille tai sementtipastalle. Myöhästyneen ettringiitin muodostuminen ei ole mahdollista, jos lämpötilarasitus kestää yli 2 päivää ja sitä ei seuraa vesisäilytys.

Kohoneen lämpötilan vaikutuksia sementtipastaan tutkittiin kokeellisesti. Kokeissa käytettiin tavallisesta ja sulfaatinkestävästä sementistä valettuja kappaleita, jotka sijoitettiin lämpötiloihin 95 °C, 175 °C ja 345 °C 124 päivän ajaksi. Osa kappaleista pidettiin myös välillä huoneenlämpötilassa, vesisäilytyksessä tai 45% suhteellisessa kosteudessa. Kappaleille tehtiin huokoisuus- ja puristuslujuuskokeet sekä termovaaka- ja röntgendiffraktioanalyysi. Portlandiitin väheneminen ja kalsiitin lisääntyminen havaittiin analyyseista altistuslämpötilan kasvaessa. Myös huokoisuus kasvoi lämpötilan mukana. Altistuminen 345 °C lämpötilaan laski sementtipastojen puristuslujuutta 20-30%. Huokoisuus- ja puristuslujuuskokeiden vertailu osoitti, että tavallinen portland sementti kesti paremmin lämpötilarasitusta kuin sulfaatinkestävä sementti.

Ikääntymistä simuloitiin numeerisella mallilla, joka implementoitiin Crunchflow-ohjelmaan. Simuloinnin tuloksia verrattiin kokeellisesti määritettyihin arvoihin. Yhtäläisyyksien lisäksi arvoissa havaittiin myös eroavaisuuksia, joten lisätutkimukselle on tarvetta. Simulaatioita tehtiin myös yhden ja kahden vuoden aikavälille. Laskentojen mukaan lämpötilassa 345 °C melkein kaikki sementtihydraatit ovat hajonneet ja vain dikalsiumsilikaattia on jäljellä.

Laskentojen ja kokeellisten tulosten mukaan 95 °C ei ole haitallinen sementtipastalle. 175 °C lämpötila ei ole haitallinen lyhyellä altistuksella, mutta esimerkiksi vuoden jälkeen melkein kaikki kalsium-silikaatti-hydraatti on hajonnut. 345 °C lämpötila on vaarallinen lyhyilläkin altistusajoilla. Laskennoissa ei huomattu eroja tavallisen ja sulfaatinkestävän sementin välillä.

Avainsanat sementtipasta, kohonneet lämpötilat, simulointi

Acknowledgements

This study has been carried out in the laboratory of Structural Engineering at the Aalto University, School of Engineering. The study was funded by the Finnish Nuclear Management Fund (YVR), the Finnish Funding Agency for Technology (TEKES), and the Academy of Finland. I thank Professor Jari Puttonen for giving me this subject and the opportunity to do my master's thesis study. I am grateful to Lic. Sc. (Tech) Olli-Pekka Kari for his guidance throughout the work. The laboratory experiments would not have been possible without the assistance of laboratory personnel, and I thank them all for their help. I would also like to thank Merja Tanhua-Tyrkkö (VTT) of her help with CrunchFlow-program and simulations.

Finally, I would like to thank my family and friends for their support during this work.

Emma Skantz

Contents

1 Introduction

1.1 Background

Normally, concrete structures are at room temperature or below it, but particularly in industrial applications as nuclear facilities it is possible that temperature exceeds a typical room temperature. The rise of temperature can be occasional or last a longer period and this rise may affect concrete chemically or physically. At high temperatures, cement minerals start to decompose, which changes the properties of cement phase. This affects also the porosity of concrete. Uneven temperature may even cause the movement of moisture in concrete leading to micro-cracking.

The standard of concrete containments (ASME), limits the temperature for concrete structures below 65 °C, except locally in normal operation or long-term period temperature can be up to 95 °C. In accidental situations or other short-term periods, the limit is 175 °C for the interior surface, and locally, the limit is 345 °C (for example caused by the steam of water).

The long-time studies about the effects of moderately high temperatures on concrete and cement paste were hardly found. There are only studies about one or few effects of high temperatures (70 °C - 400 °C) on concrete, but not any which would summarise several deterioration mechanisms caused by elevated temperature. There has neither been any modeling or predicting of the behaviour of concrete structures in elevated temperatures. Usually studies about concrete and high temperatures are done by exposing samples to high temperature for short time, such as from one hour to the maximum of two days. To find the long term effects of elevated temperature on concrete, it would be important to expose samples to temperatures for a longer period of time and study the phenomena which cause the deterioration of concrete. Modelling combined with experimental studies are essential tools to find and understand those phenomena, and which also makes it possible to forecast the behavior of concretes and cement pastes.

Even though the title of this study contains words “cement paste”, literature review discusses also concrete with cement paste. The experimental work of this study was performed with cement paste as the methods used suit better to cement paste without

aggregates. Compared to concrete, a pure cement paste is also simpler to apply the experimental results to simulation and even to build a model, since there were only cement minerals to concern.

1.2 Objectives

The main object of this work was to study the effect of chosen elevated temperatures (95 °C, 175 °C, 345 °C) on cement paste and build a numerical model for forecasting long-term effects of the temperature rises. Laboratory tests are performed and the results are used to compare with the results from numerical model. The water-to-cement -ratio and curing conditions were kept constant and two kinds of cements were chosen, ordinary portland cement (OPC) and sulphate-resisting portland cement (SR-cement) which both belong to class CEM I. SR-cement was chosen together with ordinary Portland cement since structures in industrial applications are quite often cast with sulphate-resisting cement type as it is known to be more resistant against external stresses, such as chlorides and carbon dioxide. Temperatures chosen were according to standard for concrete containments (ASME).

1.3 Contents

At first, the hydration of cement and the composition of cement paste are discussed, to have better understanding of things studied later. The basic cement chemistry is studied, that it is possible to understand the changes in cement paste caused by elevated temperature, to have the “normal” or “usual” situation to compare to. After that, various deterioration ways of concrete and cement paste caused by elevated temperatures are studied and the results from the previous studies are presented. Experimental work and the results from it are presented in Chapter 4. The numerical model and the results from the simulations performed are discussed in Chapter 5. Chapter 5 also includes comparisons between the simulations and experimental work. Error analysis from experimental work and simulations are presented in Chapter 6 following the conclusions in Chapter 7.

2 Cement composition and hydration

2.1 Clinker phases

Cement is formed during the clinkering process and the main mineral phases that cover 90% of cement are alite, belite, celite and calcium-aluminate phase. They are the 'major constituents' of cement and the rest 10% are known as the 'minor constituents'. 45 % of clinker is composed of alite (C_3S, $3CaO \cdot SiO_2$). The alite behaves with water very much similar to the behaviour of ordinary potland cement (OPC) with water. This is due to alites domination role in OPC. When water is added to alite, setting and hardening happen within few hours. If water is present, the strength increases until the age of 7 – 10 days. The compressive strength of alite is comparatively high (few tens of MPa). The hydration process of alite, as with other phases, is exothermic. For belite (C_2S, $2CaO \cdot SiO_2$), setting and hardening is slow: hardening may take weeks or even months, but the resulting strength is like with alite. Tricalcium aluminate (C_3A, $3CaO \cdot Al_2O_3$) reacts rapidly with water and the amount of heat liberated in reaction is quite high. The ultimate strength is gained in a day or two, but it is relatively low. Celite (C_4AF, $4CaO \cdot Al_2O_3 \cdot Fe_2O_3$) is regarded as an iron-bearing phase of clinker. It also reacts quite rapidly with water and strength development is fast, but the ultimate strength low. The grey color of cement is due to celite. (Soroka 2004)

The minor constituents in clinker are gypsum, free lime, periclase and alkali oxides. Gypsum is added to clinker during the grinding to retard the fast setting of C_3A. It reacts with C_3A to produce ettringite. This formation of ettringite prevents the direct hydration of C_3A and the fast setting. The optimum gypsum content depends on the C_3A content, the alkali oxides contents and the cement fineness. A large gypsum content may cause cracking and deterioration in a set cement, so the amount of gypsum must be limited. The cracking is due to the formation of ettringite, since the volume of ettringite is larger than the volume of its reactants. When only a small amount of gypsum is added, the reaction producing ettringite takes place as cement or concrete is still plastic. Standards specify the maximum amount of gypsum, which depends on the cement type and its amount of C_3A. The optimum gypsum content is temperature-dependent. It increases with the increasing hydration temperature, since the hydration of C_3A would happen faster in higher temperatures. As the optimum gypsum content is temperature-

dependent, the harmful effect of elevated temperature to compressive strength may be partly explained by the gypsum content. (Soroka 2004)

65 % of raw material used to produce Portland cement consists of lime (CaO). On clinkering, lime reacts with other raw materials, but small amount of lime may remain unreacted. As lime is intercrystallised with other minerals, it is not in contact with water. Hence, the hydration of lime occurs after the cement has set increasing also the volume of cement paste, it may cause deterioration and cracking. Even though the hydration of lime is slow, the free lime content in clinker must be limited. (Soroka 2004)

Periclase or magnesia (MgO) is produced when, a raw material of clinker, magnesium carbonate, is burn. Magnesia does not combine with other oxides of the raw material, but mostly crystallises to the mineral called periclase. Periclase reacts with water very slowly at the ordinary temperatures. The hydration of periclase to brucite increases the volume as well, so the amount of MgO in cement is limited. The alkali oxides (K_2O, Na_2O) are introduced to cement from clinker raw materials. They may react with aggregates in concrete and cause expansion if aggregates are alkali-reactive. The expansion may be avoided by using low-alkali cement, where the total alkali content is restricted. (Soroka 2004)

Clinker phases discussed form the mineral composition of cements. Cement can also be determined by its chemical composition. From chemical composition, the mineral composition can be calculated by using the famous Bogue equations. The method is not accurate since it assumes pure compounds. More accurate method to determine the mineral composition is, for example, quantitative X-ray diffraction. (Ramlochan 2010)

2.2 Interesting cement types relative to this work

As discussed earlier, the quality of cements is mainly determined by the major mineral phases of the clinker. The strength development at the later ages is mainly determined by the calcium silicates, i.e. alite and belite. Since C_3A and C_4AF have harmful effects on cement (for example low sulphate resistance), it is useful to restrict the amount of them and increase the amount of calcium silicates.

Cements used in laboratory experiments and in calculations in this work are ordinary Portland cement (OPC) and sulphate resistant Portland cement (SR-cement). It has been

noted, that cement is vulnerable to sulphates and that the vulnerability depends on the C_3A content. To produce SR-cement, the C_3A content must therefore be restricted. Even though C_4AF also makes cement non-sulphate resistant, its effect is much lesser than the effect of C_3A and the amount of C_4AF does not need to be restricted. Since C_3A reacts very quickly with water and its heat of hydration is high, the reduction of C_3A reduces also the heat of hydration of cement and slows down the rate of strength development. (Soroka 2004)

2.3 Hydration

Hydration reaction happens by mixing anhydrous cement with water. Cement paste is hardened cement, or cement mixed with water with right proportions so that setting and hardening may occur. Setting is stiffening of cement paste without significant increase in strength and it may happen within few hours after mixing cement and water. Hardening is a slower process than setting and it means development of compressive strength. Curing means storage in such conditions that it is possible for hydration to happen, for example in moist room or under water after 24 h of mixing cement and water. (Taylor 1997) The mechanisms of cement hydration discussed in this chapter can be applied to OPC and SR-cement.

The reaction of alite and belite (in cement) with water produces mainly calcium hydroxide ($Ca(OH)_2$, portlandite) and nearly amorphous calcium silicate hydrate, C-S-H gel. It has been shown, that about 70 % of alite in cement reacts in 28 days and nearly all in one year. Belite reacts slower: about 30 % is reacted in 28 days and 90 % in one year. It also produces less portlandite than alite. (Taylor 1997) A total of 40 % of hydration products of alite is portlandite. Same value for belite is 18 %. (Soroka 2004)

C-S-H is the main hydration product in cement paste. Together with pore fluid it forms a rigid gel. (Ramlochan 2010) The structure of C-S-H-gel is not totally known. It has been suggested that it is like minerals tobermorite and jennite but compared to them C-S-H-gel has many imperfections and irregularities. This makes it nearly amorphous or, in other words, it does not have clear mineral structure. (Chen et al. 2004, Jennings 2000) C-S-H-gel is mostly responsible of the engineering properties of concrete because of its continuous layered structure that binds together the original cement particles. All

the other minerals are discrete crystals and they do not form strong connections between solid phases. (iti.northwestern.edu/cement)

Other hydration products of cement paste are AFm (Al_2O_3-Fe_2O_3-mono) and AFt (Al_2O_3-Fe_2O_3-tri) phases. The most common AFm phase is monosulphate, which tends to occur at later stages of hydration. Ettringite is AFt phase, since it contains three (t-tri) molecules of anhydrite and monosulphate is an AFm phase since it contains one (m-mono) molecule of anhydrite. Monocarbonate is likely to be produced if there is present fine limestone. Limestone can be in cement or in aggregates in concrete. Other AFm phases are hemicarbonate and hydroxyl-AF. (www.understanding-cement.com)

Ettringite, which is formed at the early stages of hydration, is gradually placed by monosulphate. This is due to the increasing alumina to sulphate ratio, because of the processing hydration. On the first contact with water, most of the sulphate is ready to dissolve, but most of the C_3A is situated inside the cement grains with no initial access to water. The alumina amount decreases and the proportion of ettringite decreases as that of monosulphate increases, as the hydration continues. (www.understanding-cement.com) According to XRD-studies (X-ray diffraction) of the hydration of Portland cement, ettringite is detected within few hours after adding water to cement. The intensity of the ettringite peak reaches its maximum at the age of one day and after that weakens and may ultimately disappear. At the same time, the peak of monosulphate appears and becomes stronger. This behaviour can be seen at least in cement pastes prepared in laboratory where the CO_2 is excluded. (Taylor 1997)

However, the AFm phase formed from ettringite will be monosulphate, if the ratio of effective SO_3 to Al_2O_3 is 1. If the ratio is high, all of the ettringite will not disappear and if the ratio is low the monosulphate may undergo an anion exchange, leading to a solid solution. When considering the sulphate resistant Portland cement, ettringite has been noted to be present even until the age of 1 year, but eventually to disappear, but still monosulphate will not be seen. (Taylor 1997)

When analyzing the cement samples taken from structures, ettringite is commonly seen, but monosulphate rarely. It is possible for ettringite to persist even at the low SO_3 to Al_2O_3 ratio, as the reaction between monosulphate and CO_3^{2-} from carbon dioxide of air

products ettringite and hemicarbonate. Further reaction of hemicarbonate and CO_3^{2-} results to monocarbonate and since, the AFm phases are destroyed. (Taylor 1997)

Hydrogarnet is a result of ferrite or C_3A hydration. It has a range of compositions, C_3AH_6 is the most common phase. (www.understanding-cement.com)

It has been noted, that the hydration reaction takes place mainly at the surface of cement grain. Because of that, the hydration products are situated around the cement grain and form a capsule around it. Since hydration requires water, the rate of hydration decreases as the layer of hydration products thickens. This is due to the decreasing diffusion of water through the layer of hydration product which thickens as the hydration reaction goes on. This explains the point after which the rate of hydration decreases over time. The layer of hydration products can even reach the thickness to cease the hydration even if there are enough water present. This explains the importance of the size of cement grains and there are restrictions in standards for their minimum specific surface area. (Soroka 2004) Hydration products forming around cement grain is schematically described in Figure 1 (Brown 2010).

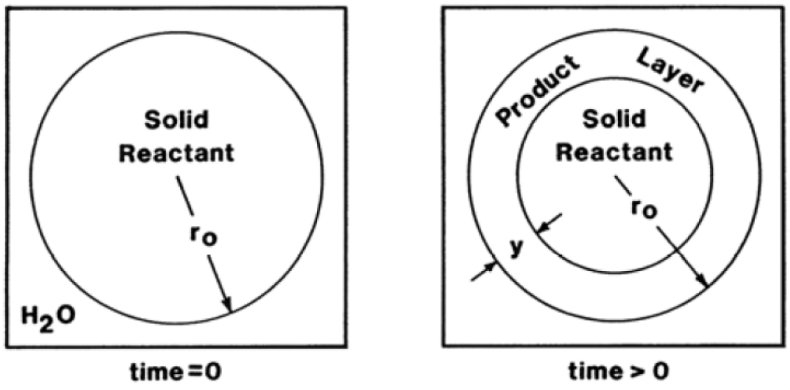

Figure 1 The formation of hydration products around cement grain. Time = 0 means the situation directly after mixing the cement and water and no hydration has happened. After that, a layer of hydration products starts to form around the cement grain. (Brown 2010)

As the volume of the hydration products is about 2,2 times greater than the volume of unhydrated cement, the distance between cement grains increases when the hydration proceeds. The hydration reaction can be divided into three stages: early, middle and later hydration. At the early stage of hydration a membrane has been noted to form over the cement grains. The composition of membrane depends on the grain, but it is mainly of alumina and silica including also significant amounts of calcium and sulphate. Also AFt phase is present on the surface of grain which occurs approximately 10 minutes

after mixing. For some time water is also around the cement grains making the paste still plastic and workable. During the middle stage of hydration about 30 % of cement hydrates. This period counts ages from 3 h to 24 h. At this stage the heat evolution is fast and C-S-H and $Ca(OH)_2$ form rapidly. The formation of C-S-H and portlandite around cement grain is illustrated in Figure 2. C-S-H forms as a membrane over the cement grain and perhaps takes over some AFt phase. Studies have shown that a gap develops between the cement grain and hydrated material. The gap is possibly filled with solution and of ions which may dissolve through the hydrated material which is porous at this time. After some time, the distance between cement grains increases as the amount of hydration products increases. The paste is no longer workable or plastic and its initial set is achieved. At the end of the middle period, AFt crystals start to grow again. As hydration proceeds, bonds begin to form at the interfaces of hydration products of the cement grains making the paste continuous.

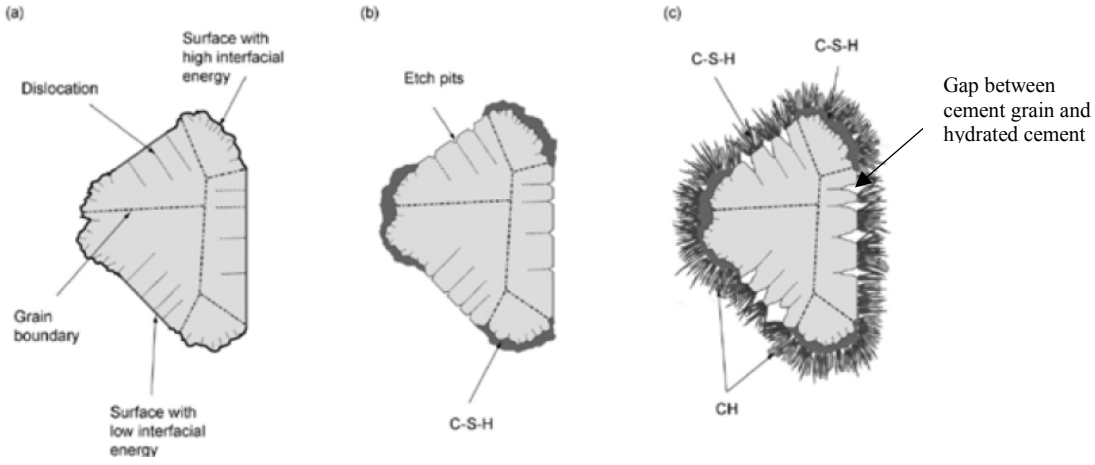

Figure 2 Formation of C-S-H-gel around cement grain (Ramlochan 2010)

Also the gaps between the grains begin to fill over the cement grains since the layer of C-S-H becomes thicker and diffusion through it decreases. This causes the stiffening of paste leading to porous solid. This continuous pore system creates capillary porosity of the paste. After the gaps have been filled, the hydration reaction slowly continues as topochemical reaction. If water is present, hydration can go forward and decreasing the capillary porosity and increasing the strength. (Taylor 1997, Soroka 2004) The C-S-H, which is formed around the cement grains, is called the ‘inner product’ or ‘inner C-S-H’, and the hydration product which is formed in the gaps initially filled with water is

called the 'outer product'. (Ramlochan 2010) As a conclusion, the summary of different phases in clinker and the following hydration products are presented in Table 1.

Table 1 Summary of the clinker phases

Clinker phases	Relative amount (Ramlochan 2010)	Hydration products (Brown 2010)
Alite C_3S	50 – 75 %	Portlandite$Ca(OH)_2$ Calcium-silicate-hydrate, C-S-H-gel
Belite C_2S	5 – 25 %	Portlandite$Ca(OH)_2$ Calcium-silicate-hydrate, C-S-H-gel
Celite C_4AF	5 – 15 %	Ettringite
Tricalcium aluminate C_3A	5 – 10 %	Ettringite (with gypsum) Hydrogarnet
Gypsum	5 – 15 %	Ettringite (with C_3A)
Free lime CaO		
Periclase		
Alkali oxides		

2.4 Porosity and water in hardened cement paste

As discussed earlier, the main hydration products of cement are calcium silicate hydrates (C-S-H), which produce a porous solid because of its randomly layered structure. This porous solid is called a gel which consists of solid particles and cohesion forces between them. The gel is unstable disintegrating in the presence of water. Set cement, however, is stable in water, which is due to the chemical bonds between particles. The strength of these chemical bonds depends on the particle size of cement gel. The greater the specific surface area of the particles is, the greater the strength of the bonds is. The mechanical strength of the cement gel is partly related to the particle size. (Soroka 2004)

The hydrated cement gel has a characteristic gel porosity of 28 % (Taylor 1997, Soroka 2004). The gel pores are relatively small compared to capillary pores. The volume of the capillary pores (remains from the originally water filled space) varies and it depends on the water to cement ratio and the degree of hydration. (Soroka 2004) Figure 3 presents the capillary porosity of hardened cement paste as a function of water-to-cement ratio. For example, if water-to-cement ratio is 0,45, the capillary porosity is 14 % (Brown 2010). The size of gel pores is some few 10s of nanometers and that of

capillary pores about 100s of nanometers. The total porosity of cement paste can be up to 50 %. (Ramlochan 2010)

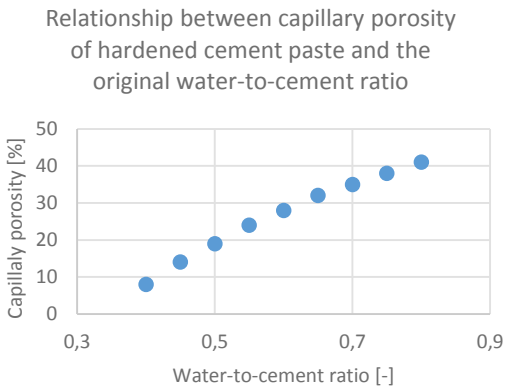

Figure 3 Capillary porosity (% per volume) as a function of original water-to-cement ratio (Brown 2010)

As set cement is porous, the amount of water depends on the surrounding relative humidity (RH). In cement paste water exist in many forms. The chemically bound water is combined in the hydration products. Water which is present in gel pores, is referred as the gel water. This water is not chemically active and is considered to be physically bound water, since the gel pores are such small that water is held in them by surface forces. The water present in the larger pores is called free water or capillary water. (Soroka 2004)

If a cement paste sample is dried at the temperature of 105 °C, the free water and gel water can be released. This way, the gel water and capillary water can be classified as evaporable and the chemically bound water as non-evaporable water. (Kontani et al. 2010) There are represented the phases of cement before hydration and during hydration in Figure 4. A schematic description of concrete, which contains aggregates, free water, cement paste, pores, and free water is given in Figure 5 where the distribution between evaporable and non-evaporable water is also illustrated.

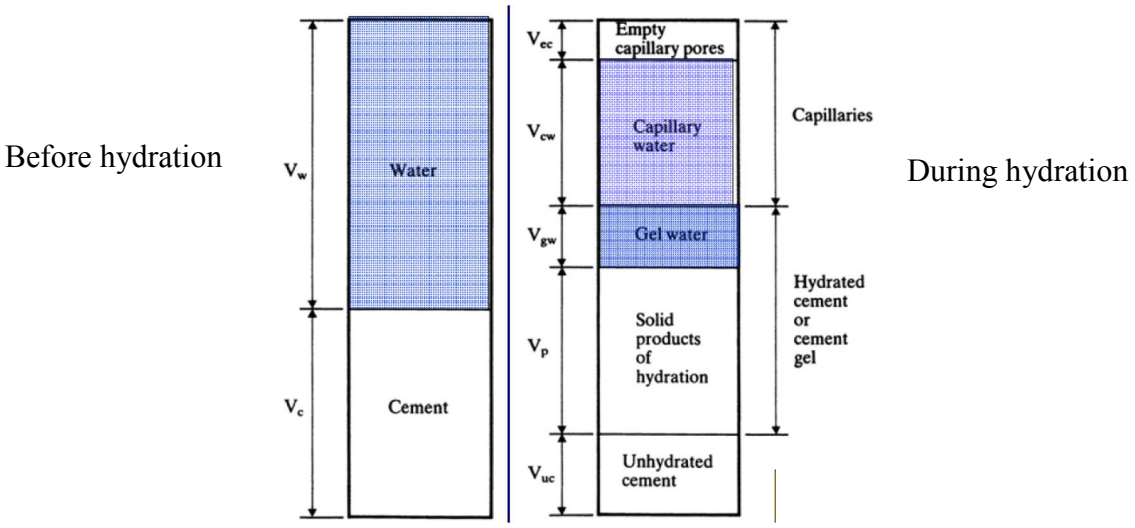

Figure 4 Representation of volumetric proportions of cement before and during hydration (Brown 2010)

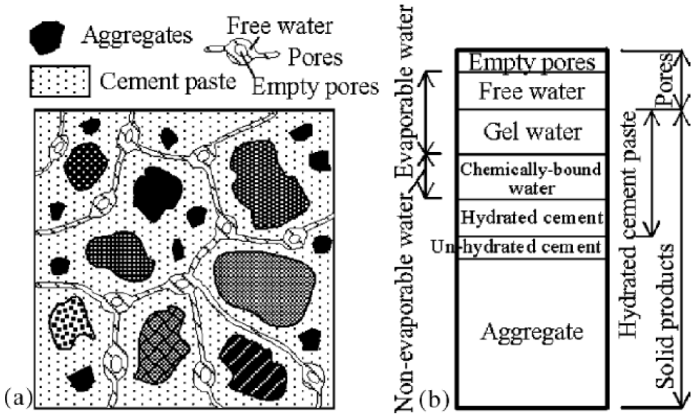

Figure 5 (a) Schematic picture of concrete containing aggregates, cement paste, air and water, (b) volumetric proportions of concrete (Ichikawa et al. 2004)

The RH around the hydrated cement paste affects the setting of water in cement paste. If RH low (< 45 %), the water is bound by adsorption in pore walls. When RH is higher, extra water binds in cement paste by capillary condensation. As the RH is 0 %, also the balance water content in concrete is 0 %. The environmental RH 100 % represents the situation where all pores are filled with water in concrete. Like with other porous materials, concrete has a sorption isotherm describing the amount of water which material can bind at different RHs. The sorption isotherm has two different curves describing the drying or wetting of material. Absorption isotherm represents the change of moisture content in concrete balanced with increasing ambient RH, as desorption isotherm, describes the drying of material. If these two isotherms are drawn in the same

picture as a function of ambient RH, the desorption isotherm is always over the absorption isotherm (Figure 6). (Ljungkrantz et al. 1994)

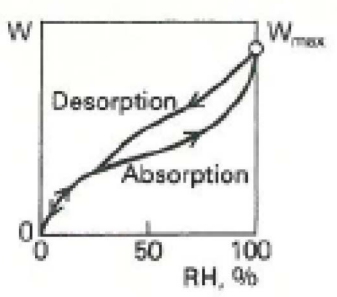

Figure 6The desorption-absorption curves of concrete (Ljungkrantz et al. 1994)

Normally concrete is not wetted or dried from total dryness or wetness. The balance between ambient RH and moisture content in concrete is determined by the history of material. Desorption and absorption always go along the curves, but the location of curves can change if the material is dried and wetted repeatedly. (Ljungkrantz et al. 1994)

The free water, which remains in capillary pores and gel pores of cement paste, provides a transport medium for ions and is called the pore solution. The composition of pore solution is affected, for example, by the type of cement, mix proportions, and aggregates. The main dissolved ions in the pore solution are K^+, Na^+, Ca^{2+}, $SO_4^{2-}$and OH^-. (Ramlochan 2010) In OPC the pH-value of this solution is typically between 13 and 14. As the pores are usually connected, the pore solution over the concrete or cement paste is also continuous which affects the transport kinetics. The irregularity of pore systems can be described by terms of tortuosity and constrictivity. Tortuosity describes, how pores are related to each other: for example, how much there are corners and other curves between the ways connecting the pores. The diffusion of gases is hindered, but, for example, the transport of ions is possible in solution offering a medium for ions and gases to transfer along the in the pore system. (Bertolinen et al. 2004)

The pore system is also the basis for other transport processes than diffusion. Species that diffuse into the concrete can bind in minerals of cement paste. For example, chlorides have been found to bind in aluminate phases or absorbed in C-S-H and carbon dioxide to bind in $Ca(OH)_2$ (carbonation). (Bertolinen et al. 2004)

In concrete aggregates are usually assumed to be stable, but that is not always the case. Since pore solutions have a high pH, sometimes the minerals in aggregates are not stable. The most common problem related to the aggregates in concrete is alkali-silica reaction (ASR). It occurs when silica dissolves in the pore water and reacts with alkalis (sodium and potassium ions) to form a gel-like coating into the aggregate particles. This gel is expansive, since it has larger a volume than its reactants. This leads to cracking of concrete. (iti.northwestern.edu/cement) ASR-reaction is controlled by the moisture level, alkali concentration in pore water, amount of portlandite, amount and reactivity of the siliceous component in the aggregate, pH of the pore solution and temperature. (Lagerblad et al. 1994) The increasing temperature accelerates chemical reactions, but for ASR-problem, the most relevant is the ultimate expansion. If there is only a small amount of reactive material, the reaction will not be able to create stresses exceeding the tensile strength of concrete. However, the ASR has been noted to process faster in the south side of the structure than in the north side. (Wigum et al. 2006)

The area between cement paste and aggregates is called interfacial transition zone (ITZ) where portlandite forms. Within the area, porosity is greater meaning that ITZ area is also weaker and the transfer of stresses from cement paste to aggregate causes micro-cracking. Locally the water-to-cement ratio is greater in ITZ-areas than in overall. (Ramlochan 2010) The reason for greater porosity in ITZ-area is that larger aggregate grains disturb the packing of smaller cement grains near the aggregates. This also leads to suggestions, that the size of ITZ-area is comparable to the size of cement grains. The limit of ITZ-area and bulk paste is not clear. As the water-to-cement ratio is increased in ITZ-areas, it is also decreased in other areas (bulk paste). For example, for a concrete, which has water-to-cement ratio of 0.4, the water to cement ratio can be reduced even to value of 0.35 in areas other than ITZ. (Scrivener et al. 2004) A greater porosity in ITZ-areas given portlandite more space to form during hydration. C-S-H-gel is distributed quite evenly between the ITZ-area and bulk cement. It has been observed that there is an increased amount of ettringite near aggregates. (Scrivener et al. 2004)

3 Concrete at elevated temperatures –effects

The increase of temperature affects concrete structures: an uneven temperature makes the moisture to move and in higher temperatures dehydration may happen affecting porosity and strength. The temperatures, which are relevant considering this work, are within the range of 25 °C – 400 °C. According to standard (ASME) about concrete containments, normally temperature should not rise above 65 °C, and locally the limit is 95 °C. In accident situations, the same limits are 175 °C and 345 °C. These temperatures were chosen in closer research. The free water in concrete evaporates when the temperature is 105 °C. Before that, approximately at the temperature range of 65 °C – 75 °C ettringite decomposes. C-S-H starts to decompose at the temperature of 150 °C. The decomposition of cement hydrates increases porosity decreasing strength. In this chapter, various deterioration ways caused by elevated temperatures are discussed.

3.1 Delayed ettringite formation

Delayed ettringite formation (DEF) takes place when ettringite is first decomposed after the cement paste or concrete has been exposed to elevated temperature and then forms again if cement paste is in water or high relative humidity. The points supporting the expansion due to later ettringite formation are:

- No expansion is observed immediately after curing at elevated temperature (65 °C or more)
- Ettringite crystals are usually present in bands around aggregate particles in concrete, which has expanded (Scrivener et al. 1999).

Because of volume change, the delayed formation of ettringite is harmful for cement pastes and concretes. Ettringite formation starts much earlier than an observable expansion (Yang et al 1999) and it has been noted that it may even happen even without clear expansion (Scrivener et al. 1999).

The delayed ettringite formation has mainly been the problem in precast concrete structures. During their manufacturing, it has been useful to heat the precast elements to accelerate the hydration which speeds up demoulding and manufacture of elements. For this reason in the most of the studies about DEF, samples are exposed to heat curing

after 2-5 hours casting, while they are still in their moulds (Lawrence 1995, Brunetaud et al. 2007, Yang et al. 1999, Zhang et al. 2002, Famy et al. 2001).

Usually ettringite is unstable at temperatures above 70 °C, but in the presence of sulphates in cement paste ettringite may be stable even at temperature of 90 °C. The reason for the disappearance of ettringite is that it competes of sulphates with C-S-H-phase and pore solutions. After the heat treatment, the sulphate coming from the decomposed ettringite is stored at the pore solutions and C-S-H-phase. The main phases that form ettringite in DEF phenomenon, when the temperature has settled, are C-S-H, monosulphate and pore solutions. (Taylor et al. 2001)

The mechanism of expansion may happen in two different ways. The first hypothesis is that relatively large crystals form at the interface of aggregates and cement paste and also elsewhere, and the pressure of forming crystals cause the expansion as they form to restricted places. The second is that much smaller crystals form within the paste and the paste expands uniformly. Both of these mechanisms have been found in studies. (Taylor et al. 2001)

Diamond (1996) and Yang et al. (1999) support the ettringite crystal pressure theory. According to their studies, the formation of ettringite has been detected in cracks around aggregates (Diamond 1996, Yang et al. 1999), where ettringite even covers aggregate grains (Yang et al. 1999). More ettringite had been found in paste-aggregate transition zone (ITZ) than elsewhere (Yang et al. 1999).

Taylor et al. (2001) suggests another expansion mechanism. After the heat treatment monosulphate is mixed with C-S-H and under expansion conditions, ettringite is also mixed with C-S-H. In Figure 7,the presence of monosulphate and ettringite with other solid phases are shown. The expansion due to the pressure of crystallisation is also demonstrated.The conditions are likely to cause pressure, since the outer product is described to be relatively dense and the amount of substances is decreasing when the distance from the inner product increases. Figure 8 shows the behaviour of cracks in concrete after heat treatment. It is assumed that expansion of cement paste produces cracks in paste and in paste-aggregate interface, when ettringite and portlandite recrystallise. The recrystallisation of these phases on crack surfaces does not affect expansion.

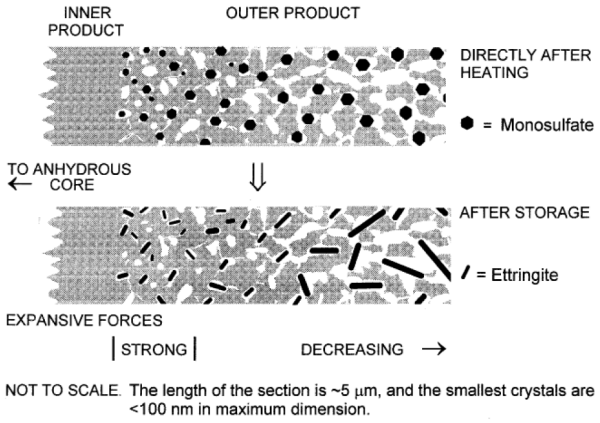

Figure 7 Schematic picture presenting the proposed model by Taylor for expansion of concrete due to the DEF. The shaded areas present all solid phases other than monosulphate and ettringite, blank areas represent pores. (Taylor et al. 2001)

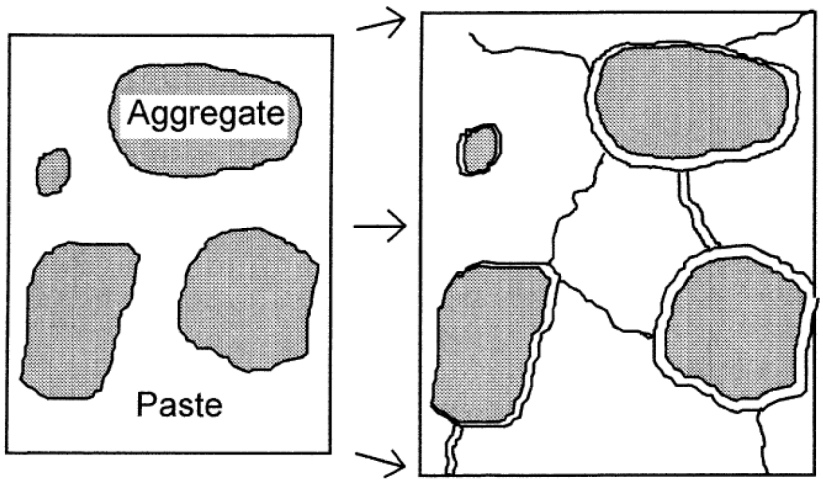

Figure 8 Schematic picture presenting the expansion by DEF according to the proposed model by Taylor. Nonuniform expansion of the cement paste produces cracks in the cement paste and also in the aggregate-cement interface. Ettringite and portlandite recrystallize in these cracks without relevant impact on expansion. (Taylor et al. 2001)

Favorable feature for cements, when considering the delayed ettringite formation is high content of C_3A and SO_3, since ettringite is formed in reaction of these two. The type III cement by ASTM contains these elements. Amount of $SO_3$is related to the gypsum content of cement. Collepardi (2003) suggests separation of the internal (sulphates coming from gypsum-contaminated aggregates or thermal decomposition of ettringite) sulphate attack and external (sulphates coming from environment; water or soil) sulphate attack. When considering the DEF expansion after heat treatment, the internal sulphate attack is usually the case.

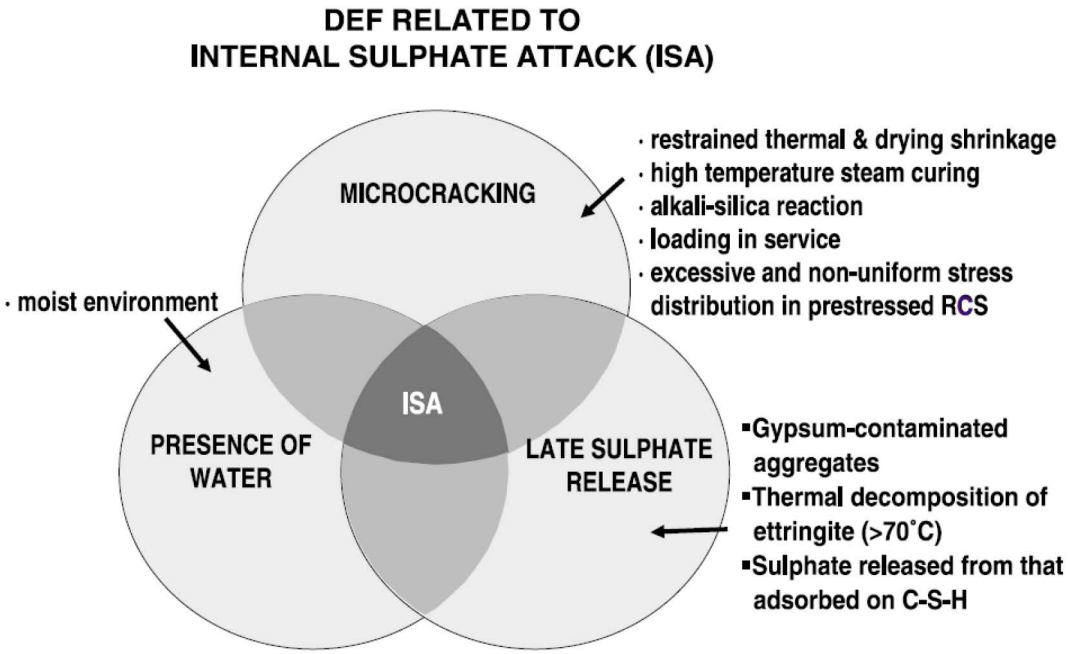

Figure 9 Essential elements to delayed ettringite formation according to Collepardi (2003)

In Figure 9, the elements related to the expansion due to the delayed ettringite formation are summarised. According to Collebardi (2003) these are the essential elements to DEF to happen and when they all are present, there is a serious risk of expansion due to the delayed ettringite formation exists. When one of these is absent, damage related to internal sulphate attack cannot occur. (Collebardi 2003)

Micro-cracking of concrete can be caused by many reasons, as noticed in Figure 9. The role of them in DEF is that, according to one theory, ettringite deposits in pre-existing micro-cracks. The late sulphate release is essential because there needs to be the reactants for ettringite to form. Reactants migrate in pore water to the micro-cracks, where ettringite can form. (Collebardi 2003)

Usually concrete samples (Brunetaud et al. 2007, Thomas et al. 2008) or mortars (Lawrence 1995, Zhang et al. 2002, Famy et al. 2001) are used for studying delayed ettringite formation, since expansion is not expected to happen in cement pastes. Also mortar and concrete specimens have been compared: the expansion was greater and faster in mortar specimen (Fu et al. 1996). This was partly explained by the higher initial curing (85 °C and 95 °C) temperatures (Fu et al 1996). It was also studied that maybe a higher cement content in mortar has an effect on expansion (Fu et al 1996). A

higher initial curing temperature might still be the issue, since when comparing mortar samples cured at the temperatures of 80 °C and 90 °C, the one cured at 80 °C did not expand after 200 days (Scrivener et al 1999). The samples cured at 90 °C expanded significantly after 200 days, but in both of them the ettringite was formed similarly after exposing to elevated temperatures and stored in water (Scrivener et al 1999). The delayed ettringite formation has also been studied (Odler et al. 1995, Yang et al 1996) in cement paste samples ending up the conclusion that it may happen, but the process is much slower than in concrete or mortar specimens. Because of that it has been noticed that presence of siliceous aggregates is not necessary for this phenomenon (Odler et al. 1995, Yang et al 1996). The cement paste samples in which the DEF was possible to detect, contained high amounts of SO_3 and C_3A (Odler et al 1995). The expansion due to DEF was also clearer in samples with high water to cement ratio and samples immersed to water after heating instead of high relative humidity (Odler et al 1995).

It has often been showed that delayed ettringite formation (DEF) requires at least temperature of 70 °C for a time long enough. The lower limit where expansion does not occur is between 65 °C and 70 °C (Lawrence 1995).Quite common temperatures which are used in DEF-experiments are 85 °C (Brunetaud et al. 2007, Zhang et al. 2002, Fu et al. 1996), 90°C (Famy et al. 2001) and 95 °C (Thomas et al. 2008). Samples are usually kept in high temperature around 2 h – 12 h. After exposure, it has been possible to detect the expansion due to the DEF for example after water storage for 650 days (Brunetaud et al. 2007) or 400-600 days (Famy et al. 2001), or keeping samples in fog room for 900 days (Zhang et al. 2002). It is important that material is kept moist or wet, temporarily or permanently, after exposing to higher temperatures. The delayed ettringite formation is slower with the material kept in moist air than with the material kept submerged (Taylor et al. 2001, Famy et al. 2001). The ultimate expansion is also smaller in moist air (Famy et al. 2001).

The type of aggregate has an influence on the phenomenon.DEF proceeds faster in concretes made of quarts aggregates than in concretes made of limestone aggregates or pure cement pastes (Taylor et al. 2001). Siliceous aggregates accelerate the expansion and it was very slow in concretes made with calcareous aggregates (Brunetaud et al. 2007). Also the type of cement affects the expansion: there were no expansion in samples made from sulphate resisting cement (Kelham 1996).

As the curing time in elevated temperature increases, the expansion behaviour requires that in addition circumstances should be appropriate for ettringite to form in cement phase (Lawrence 1995). At some heating conditions, e.g. the free aluminate/sulphate ratio may fall pass the optimum ratio (Lawrence 1995). Free aluminate is needed for formation of ettringite (Taylor et al. 2001). Extended curing at temperatures of 80 °C and 100 °C (for 3 to 28 days) resulted the absence of ettringite after 3 months of water curing at normal room temperature, whereas elevated temperature curing for 1 day and water storage after that resulted to ettringite formation (Lawrence 1995). This study was summarized so that when ettringite is seen after curing at elevated temperatures, the possibility for expansion does exist and without any ettringite, there is also no expansion (Lawrence 1995).

Delayed ettringite formation has also been used in a development of new concrete products. Shrinkage compensated cements and expansive cements are examples of products, which are based on massive ettringite formation. By adding gypsum to the cement, the expansion may be even as much as 175 % in one year. (Diamond 1996) Expansive cements can also be produced (Collebardi 2003). The hydration of calcium aluminate sulphate within few days produces ettringite, which is uniformly distributed in the hardened concrete and expands homogeneously (Collebardi 2003).

As a conclusion, the most dangerous circumstances for expansion due to delayed ettringite formation are heat treatment of 2-5 hours in above approximately 85 °C or 90 °C and after that storage in water. The samples should be mortars or concrete samples and the cement used should contain high amount of C_3A and gypsum. Also the aggregates used should be siliceous or quartz (SiO_2 or SiO_4).

3.2 Porosity

When cement paste is heated to temperatures over 65 °C, the free water from capillary and gel pores evaporates. The porosity and also the average pore size increases since heat destroys the ultrafine gel structure by dehydration. As a result of porosity increase, the bulk mass density decreases. Changes in mass density also result from thermal expansion and drying shrinkage, diffusion of water or released gases and dehydration, melting or sintering. Density of concrete is naturally also dependent from the aggregates

and their water content. (Naus 2010) The strength of the concrete is dependent from the porosity: as porosity increases, the strength decreases (Vodák et al. 2004).

The pore volume and the mean pore radii and surface have been noted to increase as the temperature increases in cement paste samples (Komonen et al. 2003). A parabolic behaviour has been detected: the specific volume of micro- and mesopores and the specific surface of pores behave parabolic in respect to temperature concluding from cement gel samples taken from concrete structures (Vydra et al. 2001). The maximum is at the temperature point of around 500 °C (Vydra et al. 2001). In mortar specimens heated to 150 °C and 250 °C , the porosity was noted to increase from the original 14 % to 15,8 % and 16,9 %, respectively (Lion et al. 2005). In cement paste, the porosity was initially 21,0 %, but after 150 °C, 220 °C and 300 °C, it was approximately 24 % (Farage et al. 2003). The increase of porosity is often explained by micro cracks (Komonen et al. 2003, Vydra et al. 2001, Vodák et al 2004, Lion et al. 2005) caused by temperature gradients. Also one reason is that pores become wider as they dry (Lion et al. 2005). Dewatering happens until a temperature of 200 °C and it also coarsens the pore size distribution (Komonen et al. 2003). It has been noted that the evaporation of free water, as the temperature is 50 °C, decreases fine pores and increases medium size pores and the evaporation of combined water. If the temperatures is 110 °C and 300 °C, large size pores are increasing (Kasami et al. 2013). After the end of dewatering, it is noted that the porosity changes originate mainly from the decomposition of cement paste components (Komonen et al. 2003). The increase of porosity within a temperature range of 80 °C – 150 °C has also been attributed to the collapse of C-S-H-gel structure (Farage et al. 2003).

Even though the porosity increases as the temperature increases and because of that the strength decreases, it was also noted that the degree of hydration has an effect on porosity after the heat treatment. The concrete samples were exposed to heating at the age of 28 d and 90 d. The maximum temperature was 280 °C. At the age of 28, heating accelerates the hydration and even the porosity increases, the strength of the concrete also increases. When the heat treatment was set to the 90 days old samples, the result was increased porosity and decreased strength. (Vodák et al. 2004)

There is a strong relation between the weight loss and porosity increase, when concrete is exposed to elevated temperatures: the porosity increases as the weight loss increases.

There are also comparisons between the weight loss and residual strength after heat treatment. The usual trend is that when the weight loss is larger, the residual strength decreases. As a conclusion the study summarises that the degradation of concrete due to the elevated temperatures is caused by the increase of pore size and volume which results in the reduction of strength, shrinkage cracks in cement paste, and cracks on interfaces around aggregates. (Kasami et al. 2013)

3.3 Dehydration

The dehydration process means decomposition of hydration products. Dehydration takes place when temperature rises above the decomposition temperature of mineral or hydrate. Theoretical decomposition temperatures and decomposition products of cement hydrates are proposed in Table 2.

Table 2 Decomposition temperatures of cement minerals

Mineral/phase	Decomposition temperature	Decomposition products
Portlandite	450 °C – 550 °C (Menéndez et al. 2012) > 200 °C (Handoo et al. 2002)	Calcite (Handoo et al. 2002) Lime (Alonso et al. 2004)
Ettringite	120 °C – 130 °C (Ramanchandran et al.) 110 °C (synthetic) (Scrivener et al. 1999)	Portlandite, calcite (Castellote et al. 2004)
C-S-H-gel	150 °C (Ramanchandran et al.)	Dicalcium silicate (Aydin et al. 2007)
Calcite	750 °C (Alonso et al. 2004)	Lime (Alonso et al. 2004)

The dehydration of portlandite was detected (Handoo et al. 2002), while heating the concrete sample from room temperature to 1000 °C. The dehydration was observed from the surface heated and also from the depth of 50 mm from surface by using XRD and thermal analysis. In the surface layer, portlandite is stabile until the temperature of 200 °C. After that, it starts to decompose, and at the temperature of 700 °C, nearly 80 % (according to the thermal analysis) of portlandite is decomposed and at the temperature range of 800 °C – 1000 °C, portlandite does not exist anymore. In the inner sample, the decomposition of portlandite is slower. It starts to decompose at the temperature of 300 °C, but there still exists some portlandite at the temperature of 900 °C (approximately

98 % of ambient portlandite has decomposed according to the thermal analysis). The XRD analysis suggests that at the temperature range of 100 °C – 700 °C, portlandite decomposes to form calcite. At the higher temperatures, calcite also starts to decompose. This is also observed from scanning electron microscope (SEM) studies. SEM migrographs taken at the ambient temperature reveals portlandite, C-S-H-gel and calcium aluminate crystals. The temperature of 200 °C did not show any change in the morphology, but at 300 °C, it can be seen that portlandite crystals are deformed and transformed to calcite. Further increase in temperature leads to development of microcracks. (Handoo et al. 2002)

Cement paste samples have been studied by neutron diffraction, thermal analysis and molecular inversion probe (MIP) analysis (Castellote et al. 2004) and XRD-analysis (Alonso et al. 2004). In experiments, the samples are under control heated to the desired temperature and then let to cool down to the room temperature before experiments. It was noted (Castellote et al. 2004) that when heating to 100 °C, the intensity of portlandite and calcite increase due to the precipitation caused by the loss of water from sample. Ettringite was found to be disappeared completely from the samples heated to 90 °C (Castellote et al. 2004), 100 °C (Alonso et al. 2004) and 200 °C (Alonso et al. 2004). In XRD-studies of concrete exposed to temperatures up to 300 °C, the peak of ettringite is seen at the temperatures of 20 °C and 50 °C, and a weak peak is also seen at the temperature of 80 °C (Kasami et al. 2013). At the temperature of 110 °C, ettringite is no longer seen (Kasami et al. 2013). The Ca^{2+} coming from the decomposition of ettringite contributes to the precipitation of portlandite and calcite (Castellote et al. 2004). The reduction in portlandite can be seen at the temperature of 450 °C (Alonso et al. 2004), and when the temperature reached 530 °C or 560 °C (Castellote et al. 2004), portlandite decomposed rapidly. At the temperature of 750 °C, portlandite is not seen any more (Alonso et al. 2004). Also C-S-H gel had been disappeared at 400 °C (Castellote et al. 2004). Calcite is present until the temperature of 450 °C, and the intensity of it even increases as the temperature increases (Alonso et al. 2004). At the temperature of 750 °C, calcite has practically disappeared and instead of that, lime is detected (Alonso et al. 2004). This is explained by the transformation of portlandite and calcite to lime (Alonso et al. 2004).

During cooling, it was noted that CaO decomposes back to portlandite with water from environment. When comparing OPC and low C_3A cement (sulphate resistant), the decomposition of CaO back to portlandite happens only partly in OPC, but it is total in low C_3A cement. According to the experiments, C-S-H gel and ettringite are not recovered after cooling, but calcite recovers. This is explained by the uptake of CO_2 from atmosphere. (Castellote et al. 2004) After heating to 300 °C and then saturating with water, cement paste samples were found to recover to their original porosity, which was explained by the rehydration of decomposed C-S-H or hydration of initially unhydrated cement grains (Farage et al. 2003).On the other hand, the porosity of cement paste samples heated to 100 °C and 200 °C and then recovered in 20 °C and RH 60 % was increased during recovering (Janotka et al. 2005). Also the compressive strength was decreased (Janotka et al. 2005). This was explained by the rapid cooling after high temperature and it was also mentioned that the "self-curing" of cement paste does not contribute to the structural improvement (Janotka et al. 2005).

3.4 Movement of moisture

Movement of moisture due to elevated temperature can result from drying from an exposed boundary or from temperature gradients and it is related to the porosity. Up to the temperatures of 400 °C, the migration of vapour is controlled by pore vapour pressures. Usually there are about 2 – 4% unfilled pores in concrete and they allow the vapour pressure to develop during heating. They also act as a reservoir of moisture and smooth the high vapour pressure and temperature. Porosity prevents the hydraulic cracks during the heating, which may happen because of the different thermal properties between concrete and aggregate. (England et al. 1995)

The migration rate is fastest where the temperature is greatest and, because of the high temperature, also the pressure is greatest. The resulting mass transfer causes saturation on the pores near the lower temperature areas. There the movement of vapour is controlled by the hydraulic pressure gradients between the two ends of the saturated area. The creation and deposition of additional hydration products are likely to happen because of the right moisture and temperature conditions of the saturated zones. This leads to reduction of permeability and hence, the reduction of moisture flow. Therefore, the moisture loss to the surroundings is dependent on the flow properties of the saturated zone. (England et al. 1995)

In Figure 10, the moisture movement is described. The boundary at the left hand side is heated and the water and vapour migration is from left to right. A pore saturation zone has been developed in the core of the wall because of the differential migration rates. If migration continues, the length of the saturation zone grows because more vapour condensates at saturation front. At this phase, four different stages can be found from the structure, as in Figure 10(d). On both sides of the saturated zones, there are partially saturated areas. Near the hot face, there is a dry zone, or superheated steam zone. As time goes on, the saturated zone moves towards the cold boundary and if it is not sealed, water can evaporate from the right hand side of the saturation plug. At the same time, vapour continues to condensate on the left hand side of the saturation plug and the zones A and B from Figure 10 (d) are enlarging. Eventually, the whole structure is partly saturated and migration continues until all water has evaporated. In a massive concrete structures, the fully evaporation of water takes years and it is not normally reached during the usual service life (for example 50 years). (England et al. 1995)

As a non-uniform temperature is affecting a concrete structure, the pore pressures in it are usually related to the vapour pressure in a partially saturated porous structure. Additional pressures are usually related to the air in pores, which is heated. Above the temperatures of 250 °C it is also possible that more gaseous phases release from composed hydration products of cement. The released water from hydration products has two effects: firstly, extra water is made available to sustain pore pressures higher than would be expected and secondly, the pore volume increases. All of these pressures have an effect on the migration process. Total pore pressure contributes to the movement of liquid water, the partial gas pressures control the mass movement of the gaseous components and the water vapour pressure control the water vapour. (England et al. 1995)

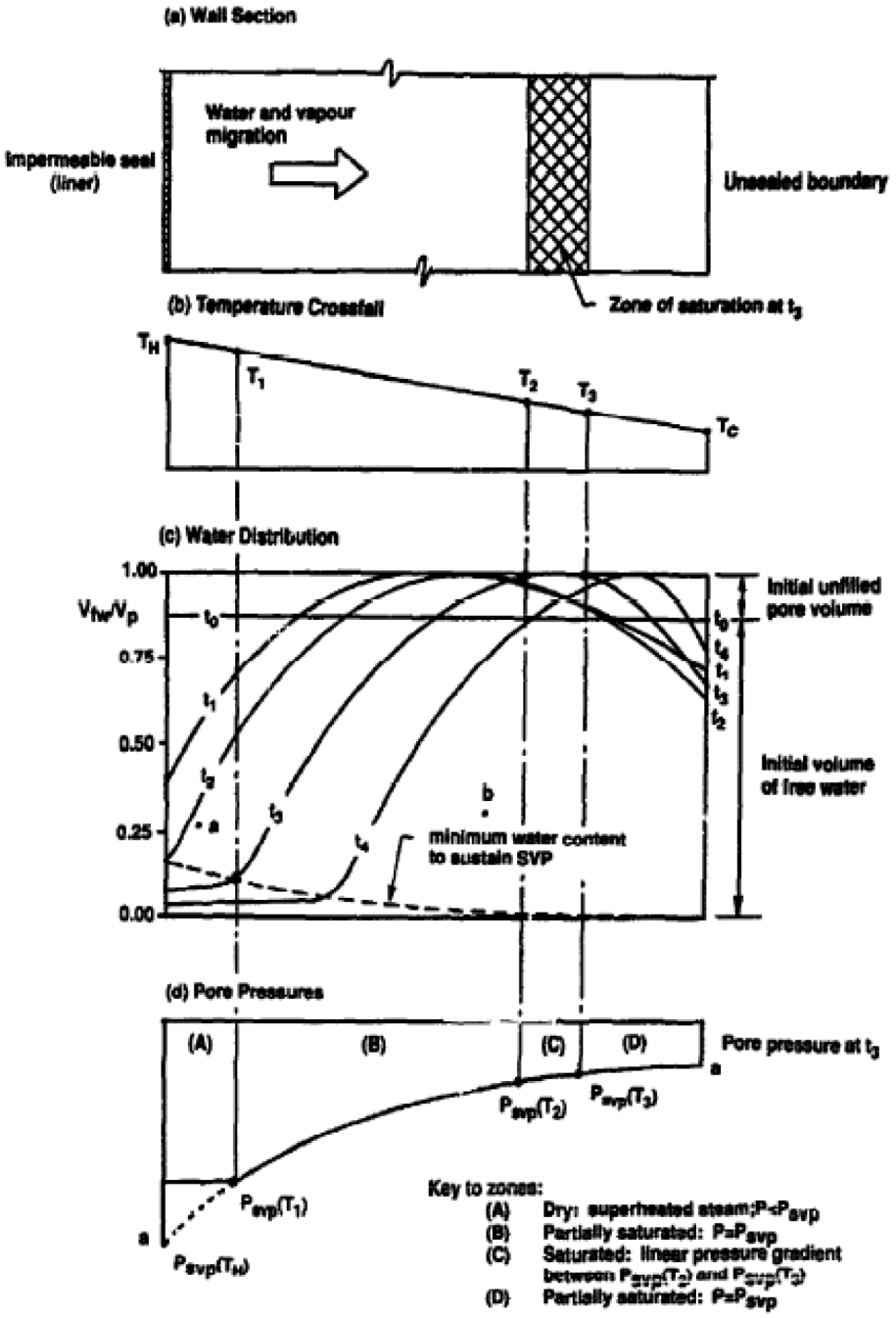

Figure 10 Schematic representation of moisture movement and pore pressure distribution in the thick concrete structure, when subjected to a temperature crossfall through its thickness (England et al. 1995)

Cement paste having low water to cement ratio may be quite dense and have quite impermeable microstructure and it is possible that it keeps the water inside even at the high temperatures. Because water cannotevaporate, it produces high internal pressure which may cause spalling. (Komonen et al. 2003) Spalling is more serious problem in

high-performance concretes than in ordinary concretes. The factor affecting the spalling is high compactness of high-strength concrete. (Kalifa et al. 2000)

Spalling of concrete is a result of two processes: the first one is the heat expansion of components (thermo-mechanical process) and the second one is associated with the mass transfer of liquid or gases in porous media (thermo-hydraulic process). These two things result in the high pore pressure and pore pressure gradients in concrete. Considering this work, the thermo-hydraulic process is more relevant since it is situated in cement paste. Thermo-mechanical process is based on the heat expansion of two different materials, aggregates and cement paste, which have different thermal properties. As aggregates expand while they are heated, cement paste shrinks as soon as it loses water (by drying and dehydration). (Kalifa et al. 2000)

The thermo-hydraulic process described in (Kalifa et al. 2000) is basically the same as the water movement discussed earlier in this chapter (from reference (England et al. 1995)). Layers in structure are also suggested to form when concrete structure is heated (Kalifa et al. 2000). A quasi-saturated layer is proposed to form behind the dry and drying layer, to which heating is directed. This quasi-saturated layer acts as an impermeable wall and prevents the transport of gases through it. The lower the permeability of material is, the sooner (and the closer to the heated boundary) this wall is generated, and also the higher the pressure and its gradient are. The difference between these two theories is that, the pressure in pores is claimed to be the biggest at the quasi-saturated area (Kalifa et al. 2000), comparing to the case (England et al. 1995), where the pressure is noticed to be biggest near the heated boundary. This difference can be seen from Figures 10 and 11.

Besides permeability, heat conductivity also affects the thermo-hydraulic process of spalling of cement paste. Also the heat and mass transfer depend on the moisture content of the material. It is noticed (Khalifa et al. 2000) that spalling is not fully deterministic phenomenon and parameters that has an effect on it also depend on each other. The model (Khalifa et al. 2000) to describe spalling is only a theoretical model. The temperature on experiments was 600 °C.

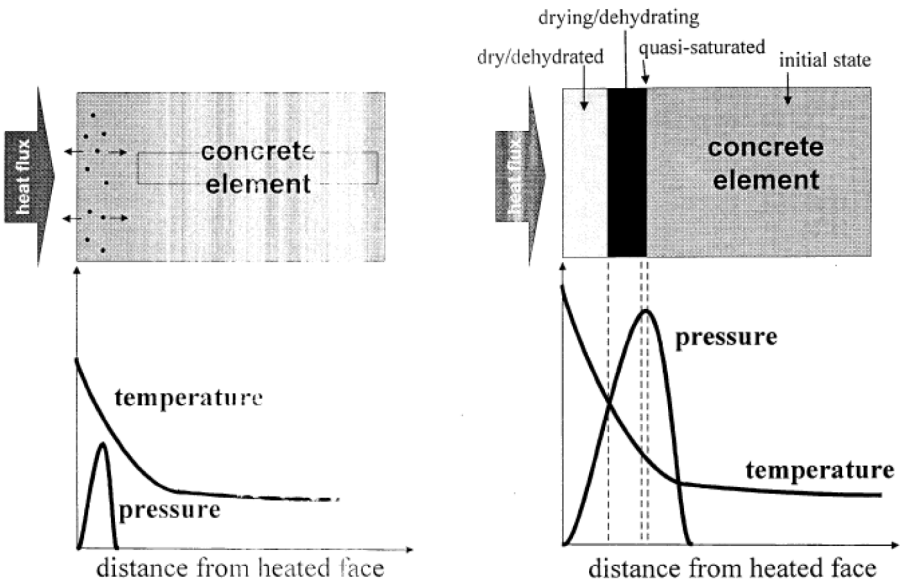

Figure 11 The process of developing of the pore pressure in concrete structure heated at the boundary. The water vaporised by the effect of heat is transported not only towards the outside, but also the inside, towards the lower temperature zones. It condensates again and quasi-saturated layer is formed which prevents the transport of mass in the inner direction. (Khalifa et al. 2000)

3.5 Drying shrinkage

The moisture content of porous concrete or cement paste has an effect on the volume. As the moisture content decreases, also the volume of the structure decreases. This is called a drying shrinkage. The increasing of the volume due to the increase of the moisture content is called swelling. Shrinkage and swelling can cause cracking to the concrete, and, thus disorientation to the structure. (Soroka 2004) Shrinkage of concrete is a result of two things: drying and autogenous volume change. Drying is more predominant of these effects. Naturally, temperature has effects on the rate and magnitude of drying shrinkage increasing them with increasing temperature. An autogenous shrinkage results from continued cement hydration which reduces the free water content. The volume of hydration products is smaller than the separate volume of components. (Naus 2010)

3.6 Carbonation

The carbonation of concrete is a phenomenon in which carbon dioxide (CO_2) from air dissolves to the pore solution of cement paste and reacts with solute portlandite ($Ca(OH)_2$). A more detail description of the process is that as the gaseous CO_2 penetrates to the pore solutions, it becomes carbon rich solution. Carbon ions

decompose from acid solution releasing protons. In this reaction, carbon rich acid neutralizes the alkalinity of pore water. Portlandite dissolves to the pore water and reacts with carbon dioxide to form calcium carbonate (calcite). The whole process is described in equation 1. (Maekawa et al., Thiery et al. 2007)

$$\begin{gathered} H_20 \leftrightarrow H^+ + OH^- \\ CO_2 + OH^- \leftrightarrow HCO_3^- \\ H_2CO_3 \leftrightarrow H^+ + HCO_3^- \leftrightarrow 2H^+ + CO_3^{2-} \\ Ca(OH)_2 \leftrightarrow Ca^{2+} + 2OH^- \\ CaCO_3 \leftrightarrow Ca^{2+} + CO_3^{2-} \end{gathered} \tag{1}$$

A more simple way to describe the carbonation reaction is presented in equation 2 (Maekawa et al.):

$$Ca(OH)_2 + CO_2 \xrightarrow{H_2O} CaCO_3 + H_2O \tag{2}$$

In carbonation reaction, mainly portlandite reacts with carbon dioxide to from calcite, but also other phases in cement paste may react. Reaction between C-S-H and CO_2 produces calcite and silica gel. It has also been noted that ettringite decomposes due to the carbonation to calcite, gypsum and aluminate gel. (Maekawa et al., Thiery et al. 2007)

Carbonation is detrimental for concrete structures, since it neutralizes the pore solutions and also causing changes in its major compounds, and pore solution and pore structure. As the pH-value drops, the passive layer around the steel reinforcement bars breaks down and this makes it possible for corrosion to happen as well. Before carbonation the pH-value of concrete or cement paste is around 12 – 13, as after carbonation it may decrease below 11. (Maekawa et al., Kari 2009)

Many things affect to the carbonation reaction. For start, reaction can happen only if there is water in concrete, but if sample is submerged or totally wet, reaction is very slow. The optimal RH for the reaction is around 60 % - 70 %. Carbonation and forming of calcite are chemical reactions and their rate is dependent on the surrounding environment. The higher the temperature is, the faster the reaction proceeds. Obviously, the carbon dioxide level in air has an effect on the reaction: the higher the level is, the faster the carbonation reaction happens. (Kari 2009)

When considering this work, carbonation is an important phenomenon since the reaction rate increases as the temperature increases. In a study (Matsuzawa et al. 2010) concrete samples were exposed to accelerated carbonation test (5 % CO_2) using different relative humidities and temperatures of 20 °C and 60 °C. It was noted, that carbonation proceeded faster at 60 °C than at 20 °C. At the temperature of 60 °C, carbonation proceeded fastest when RH was lowest (30 %), and the rate of the reaction decreased as the RH increased. This was explained by the absolute humidity, which is higher at higher temperatures than at lower temperatures despite of the relative humidity. So, it can be concluded that the amount of water in concrete is higher at the higher temperatures. (Matsuzawa et al. 2010)

When concrete structures were studied after fire, it was noted that carbonation reaction had been developed totally at the surface exposed to fire. At the inner parts of structure, crystals of portlandite were still left. However, the concrete structure studied was 15 years old when the fire damage happened and carbonation has probably proceed quite much over service life. (Georgali et al. 2005)

The effects of temperatures on concrete and cement paste discussed in Chapter 3 are summarised in Figure 12.

Temperature	Effects			
< 50 °C	Evaporation of capillary & free water (Kasami et al. 2013)	Decrease of fine pores, increase of medium size pores (Kasami et al. 2013)		
60 °C	Carbonation proceeded faster at 60 °C than at 20 °C (Matsuzawa et al. 2010)			
90 °C	Ettringite decomposition (Castellote et al. 2004)	Precipitation of portlandite and calcite (Castellote et al. 2004)		
< 105 °C	Free water and gel water is released (Ramachandran et al.)			
110 °C – 300 °C	Dehydration of cement hydrates (Kasami et al. 2013)	Evaporation of combined water (Kasami et al. 2013)	Increase of large size pores (Kasami et al. 2013)	Pore volume increases (England et al. 1995)
			Extra water sustain higher pore pressures (England et al. 1995)	
		Pore pressure is affected by the decomposition gases from cement hydrates (England et al. 1995)		
150 °C	Decomposition of C-S-H-gel (Ramachandran et al.)			
< 200 °C	Pore pressure is related to the vapour pressure (England et al. 1995)			

Figure 12 A summary of the effects of temperature discussed in Chapter 3

4 Experimental work

4.1 Materials and methods

4.1.1 Materials

The cement paste samples were cast using ordinary Portland cement CEM I and sulphate-resistant (SR) cement CEM I. The chemical composition and clinker phases of cements are given in table Table 3. The water to cement-ratio was 0,426 in both cases. Pastes were prepared according to the standard SFS-EN 193-3. The specimens prepared of each cement type were following: 7 pieces of 100 mm x 100 mm x 100 mm cubes, 15 pieces of 40 mm x 40 mm x 160 mm prisms and 4 pieces were cast in a PE-bottle. After demoulding the specimens were placed in water at the age of one day. All the specimens except those which were intended to be used in compression strength test and porosity test representing the initial stage were removed from the water storage at the age of 26 days and placed in a room of RH 45 % and temperature 20 °C. After two days the mass change was about 0,5‰ in a day, and the specimens were ready to put into the oven.

Table 3 Chemical composition, clinker phases and compression strength of cements

Chemical composition	OPC [%]	SR-cement [%]
SiO_2	19,9	19,8
Al_2O_3	4,2	3,4
Fe_2O_3	3,3	3,9
CaO	63,2	64,5
MgO	3,3	1,8
K_2O	1,3	0,4
SO_3	3,2	2,5
Na_2O	1,2	0,8
Clinker phases		
C_3S	54,7	77
C_2S	14,4	0
C_3A	5,8	3
C_4AF	6,3	12
Compression strength 28 d	[MPa]	[MPa]
	52	54 – 59

4.1.2 Porosity measurements

The porosity tests were started after the samples were kept submerged 28 days (before heat treatment).

At first, samples were dried in an oven at the temperature of 105 °C until the constant weight (smaller than 0,5‰ change in a day). After that, specimens were let to cool for one day. Then they were saturated by water in the following way: at first a container with samples was filled with water to the ¼ of the height of the samples, after 2 hours to the ½ of the height of the samples and again after 2 hours to the ¾ of the its height and after one day, samples were totally submerged. When weight did not change anymore, the porosities of the samples were calculated by equation

$$P = \frac{B - A}{B - C} \cdot 100\ \% \tag{3}$$

where P is the porosity [%],
A is oven dried weight [kg],
B is water saturated weight in air [kg] and
C is water saturated weight in water [kg] (Khan).

4.1.3 Compressive strength test

At the age of 28 days the compressive strength test was performed to specimens according to the standard SFS-EN 12390-3. Specimens were kept in a water storage until the moment of testing. Also the specimens exposed to 124 d to the temperature of 345 °C were tested.

4.1.4 Temperature tests

At the age of 28 days samples were placed in ovens. The temperatures used were 95 °C, 175 °C and 345 °C. The heating rate up to the temperature of 345 °C was approximately 3 °C/min. Because of the oven type, it was not possible to control the heating rate with the temperatures of 95 °C and 175 °C, but the heating was fast: about 10 minutes to the temperature of 95 °C and about 20 minutes to the temperature of 175 °C. Four cement paste prisms and one sample removed from the plastic bottle were placed in every temperature. A part of the samples were subjected to constant exposure of high temperatures and another part was subjected to four heating and cooling cycles. Same ovens were used in both of the cases.

The constant storage in high temperature continued 124 days. Ovens were cooled down slowly. Samples were taken for further analysis with thermal analysis and XRD.

Specimens from both cement pastes were exposed to temperature and cooling (room temperature) cycles. At the room temperature (25 °C), samples were kept either in water or at relative humidity 45 %. The duration of one cycle was approximately 20 days in high temperature and 10 days at a room temperature. After water storage, samples were first dried before heating again. In total 4 cycles between high temperatures and RH45 or water storage were performed. After the last time in water and RH 45%, samples were taken from each specimen for further analysis.

4.1.5 Thermal analysis

The thermal analysis was performed for the samples with equipment DuPont Instruments 951 Thermogravimetric Analyzer. Thermal analysis is a method for determining different minerals in cement of concrete. The results of the analysis are TG- and DTG-curves. For the analysis, a piece of each sample was taken and powdered, for having 40 mg – 55 mg of powder. Each sample was heated at the speed of 20 °C/min until the temperature was 1000 °C. When the temperature is rising, the mass of the sample is studied. TG-curve presents the percentual change in mass as a function of temperature whereas DTG-curve presents the derivative of TG-curve as a function on temperature, in other words the rate of change of the mass.

A part of each sample was powdered before they were exposed to heat treatment to represent the initial stage. Also samples were taken after 124 d in high temperatures and after four cooling and heating cycles.

4.1.6 XRD-analysis

The minerals in cement paste were determined by X-ray diffraction analysis. The equipment used was Philips PW1710 diffractometer with CuK radiation (40 kV and 40 mA).The measurements were performed from 2 angles of 5,015° to 99,965° with step of 0,03°. The result is a graph which describes the intensity on every value of angle 2θ. From this graph and comparing it to thermal analysis, an approximate amount of every mineral can be calculated.

4.2 Results

4.2.1 Compressive strength test

The results from compressive strength tests are given in Table 4. In total 3 samples were tested from both of the cement types and the result presents averages of the

measurements. At the initial stage, the results from these two cement types were quite similar, which is natural since they both belong to the group CEM I 42,5.

Table 4 Compressive strength results

Compressive strength [MPa]	Ordinary Portland cement	Sulphate resistant cement
28 d	58,3	59,1
after 124 d in 345 °C	47,9	43,2

The strength of specimens exposed to temperature of 345 °C were also determined. The results are also shown in Table 4. The strengths after temperature treatment are 82 % (OPC) and 73 % (SR-cement) from the original. The strength reduction of SR-cement was larger than that with OPC.

4.2.2 Porosity

The porosity of the initial stage was determined at the age of 28 d, which was also used as an initial value in the simulations. The porosities after exposing the samples to the temperatures of 95 °C, 175 °C and 345 °C were also studied. The results of total porosities are presented in Table 5.

Table 5 Porosity results

Porosity [-]	Ordinary Portland cement	Sulphate resistant cement
28 d	0,35	0,35
after 124 d in 95 °C	0,39	0,40
after 124 d in 175 °C	0,44	0,43
after 124 d in 345 °C	0,50	0,52

The temperature of 95 °C affected the porosity only little. In study (Farage et al. 2003), the temperature of 80 °C increased the porosity of cement paste also only from 21,0 % to 21,8 % where as when the temperature was 150 °C, the porosity had increased to the value of 24,0 %. In our study, the porosity increased more when temperature increased to 175 °C and 345 °C, which was in accordance with earlier studies (Lion et al. 2005, Farage et al. 2003). The increase of porosity was larger with SR-cement. As porosity and compressive strength are related to each other, a larger strength decrease with SR-cement can be explained by a larger porosity increase. The results from porosity tests and compressive strength tests are in accordance with each other.

4.2.3 Thermal analysis

When heating the sample in thermal analysis, at first the gel and capillary water evaporates at the temperature of 105 °C. After that, at the temperature 130 °C, ettringite decomposes and C-S-H decomposes under the temperature of 150 °C (Ramachandran et al.). The decomposition of portlandite happens at the temperature of about 450 °C and it makes a clear peak to the DTG-curve. Calcite decomposes on two stages over the temperature range of 600 °C – 700 °C. It is possible to calculate the amounts of portlandite and calcite in the samples from the thermal analysis based on the mass change and the chemical reaction of decomposition.

Figures 13-18 represent the graphs on the thermal analysis made. The temperature 25 °C (room temperature) refers to the initial samples which were taken before any heat treatment. Other temperatures refer to the exposure temperatures. The term “high temperature” in text refers to these exposure temperatures.

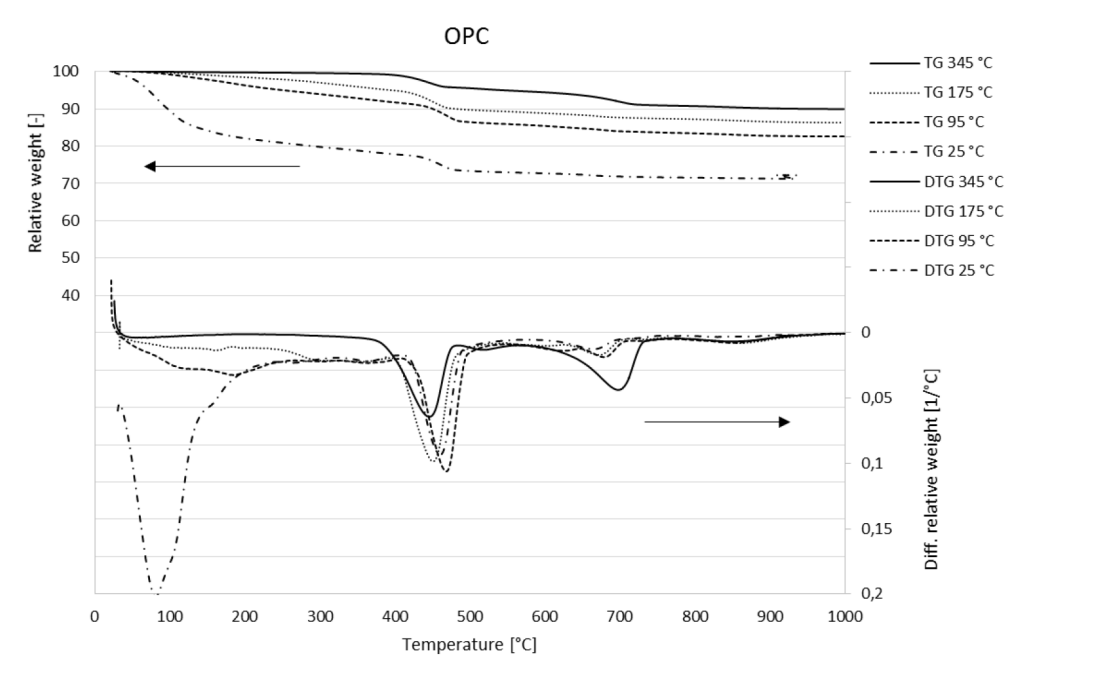

Figure 13 TG and DTG curves of OPC cement paste at the initial stage and after exposing to temperatures of 95 °C, 175 °C and 345 °C for 124 d

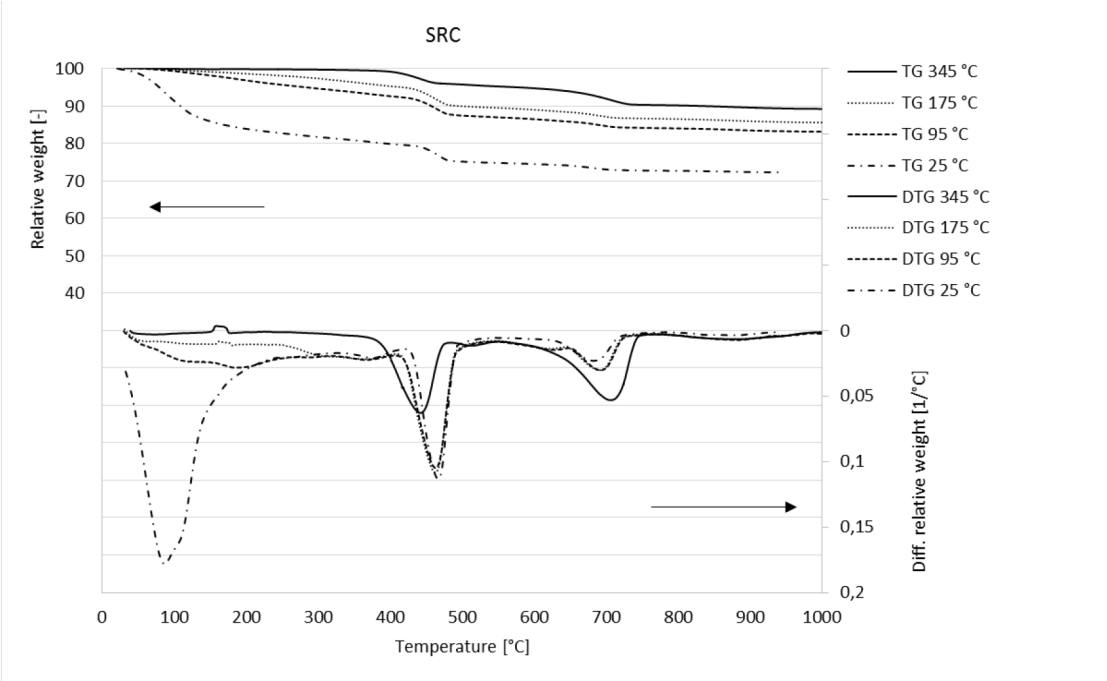

Figure 14 TG and DTG curves of SR cement paste at the initial stage and after exposing to temperatures of 95 °C, 175 °C and 345 °C for 124 d

Figures 13 and 14 show the results of the thermal analysis of cement paste samples presenting their contents at the initial stage after heat treatment for 124 d in 95 °C, 175 °C and 345 °C. The main differences between the temperatures with both types of cement samples can be found at the temperature range of 20 °C – 300 °C. This corresponds to the evaporation of free water and decomposition of ettringite and C-S-H-gel. At the initial stage, the peak at this range is largest since there is still water to evaporate. In the samples treated in 95 °C the peak at this temperature area can still be found, which would correspond to that there is still at least some C-S-H-gel left since the decomposition temperature of ettringite in cement is lower than that of C-S-H (Ramlochan 2010). In samples treated in 175 °C, the peak of etringite and C-S-H-gel has almost disappeared. This can also be seen from the TG-curves, since it is almost straight between the temperatures of 20 °C and 300 °C. There are differences between the second peaks of the DTG-curves: the portlandite amount is quite same in the initial samples and samples treated at 95 °C or 175 °C, but in sample treated at 345 °C the amount of portlandite has decreased. Same observations can be found elsewhere (Handoo et al. 2002). There are also observations (Handoo et al. 2002) that portlandite decomposes to transform to calcite. The last peak represents the calcite amount increased with the temperature, which is in accordance with decreasing of portlandite.

In both cement samples, which are treated in 345 °C, there happens some decomposition at the temperature range of approximately 500 °C – 550 °C. This may reflect to the decomposition of dicalcium silicate, which has formed as the C-S-H has decomposed (Jernejcic et al. 1977).

In Figures 15 and 16, the results of the thermal analysis from the samples, which were exposed to high temperatures and cooling cycles in RH 45 % are given. Similarity as with samples exposed to a constant high temperature can be seen: increasing the exposure temperature has decreased portlandite amount and increased calcite. In both cement samples exposed to 175 °C and 95 °C, the decomposition of calcite happens in two steps, which can be seen from the DTG-curves.

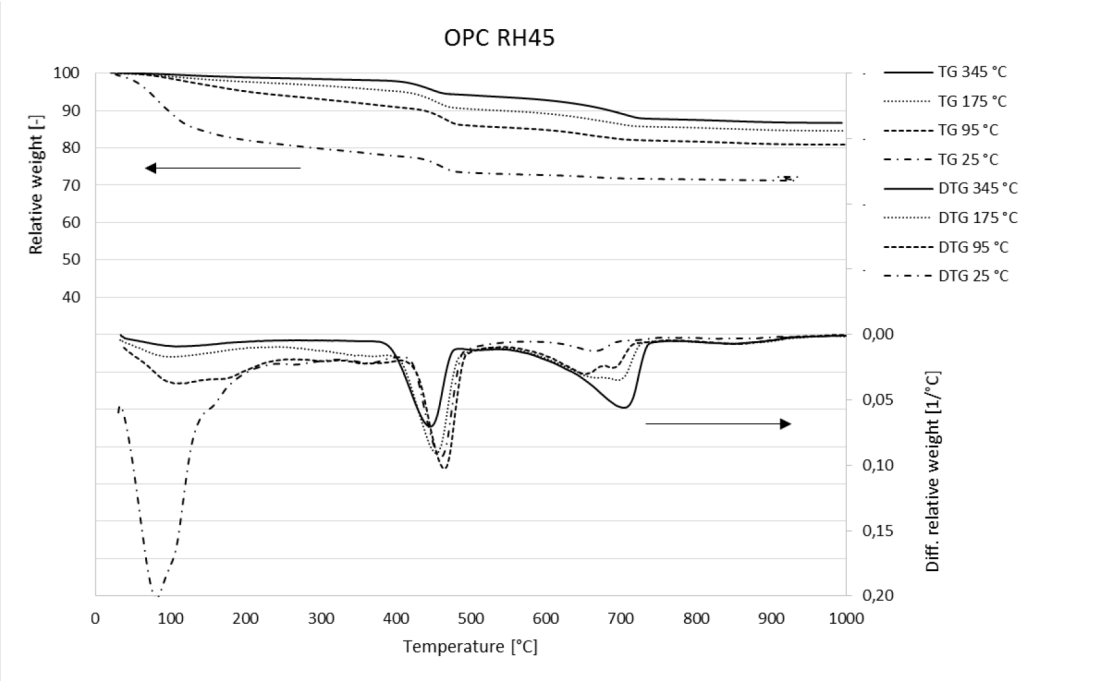

Figure 15 Thermal analyses from the initial stage of OPC and samples exposed to 4 temperatures and cooling cycles in RH 45 % (temperatures 95 °C, 175 °C and 345 °)

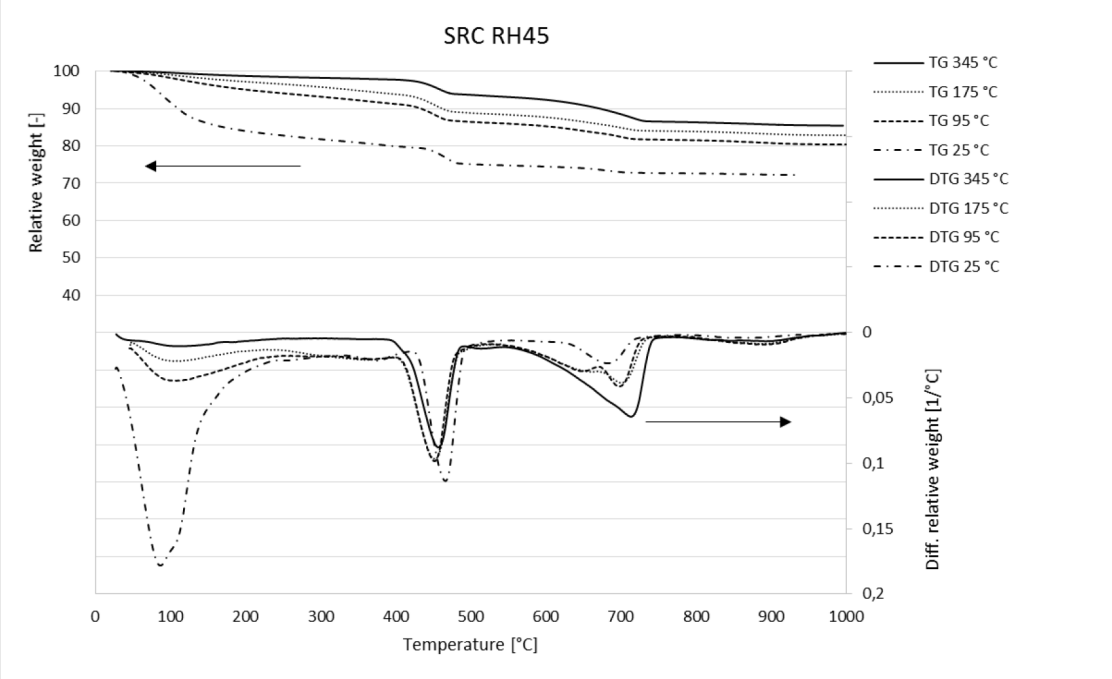

Figure 16 Thermal analyses from the initial stage of SR-cement and samples exposed to 4 temperatures and cooling cycles in RH 45 % (temperatures 95 °C, 175 °C and 345 °)

In Figures 17 and 18, the results of thermal analysis made for the samples exposed to high temperature and water cycles are represented. When considering the OPC, the effect of temperature on the results is minor. Portlandite amount has slightly decreased and calcite amount increased in high temperatures. In SR-cement sample, the effect of exposure temperatures is also quite small. Larger changes can be seen in DTG-curves at around the decomposition area of C-S-H and ettringite. This can also be connected to the amount of water saturated in cement paste samples.

The similarity of samples exposed to different temperatures may be explained by dehydration. It has been noticed, that portlandite and calcite recovers after heating and water storage (Castellote et al. 2004).

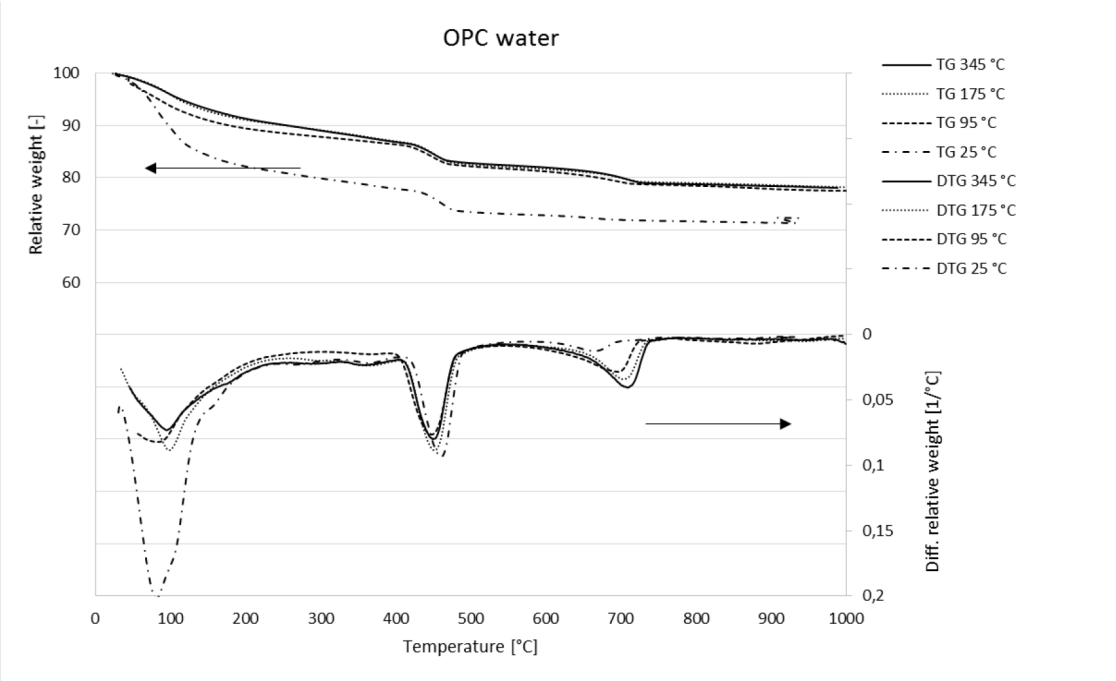

Figure 17 Thermal analyses from the initial stage of OPC and samples exposed to four temperatures and cooling cycles in water (temperatures 95 °C, 175 °C and 345 °)

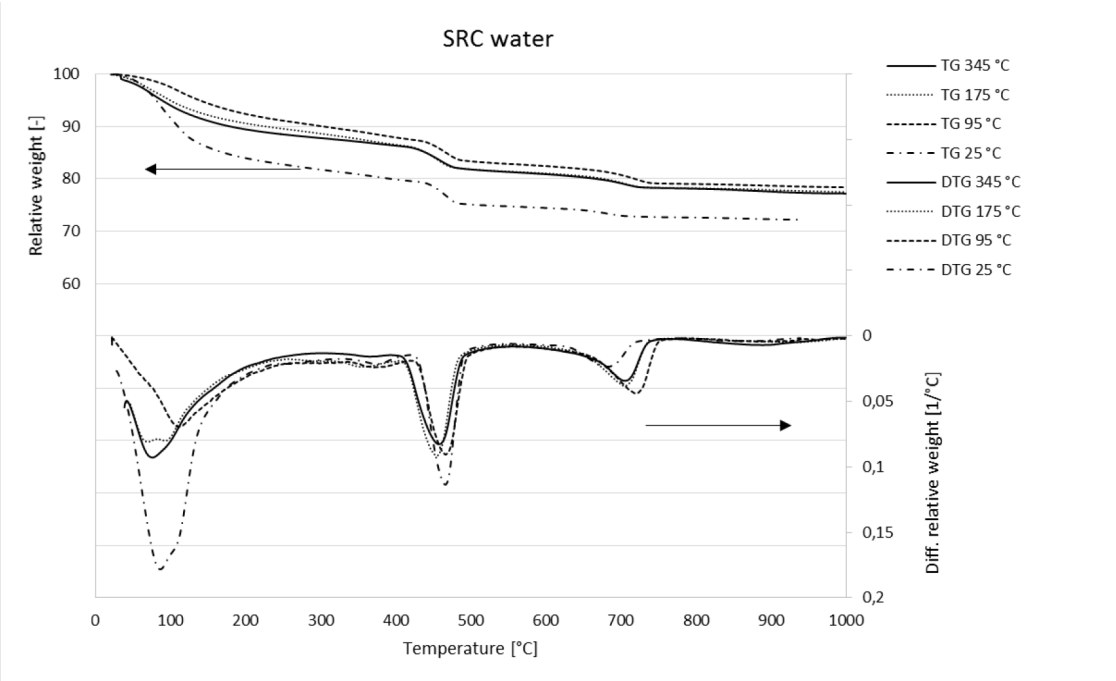

Figure 18 Thermal analyses from the initial stage of SR-cement and samples exposed to four temperatures and cooling cycles in water (temperatures 95 °C, 175 °C and 345 °)

4.2.4 XRD-analysis

XRD-analyses were carried out after taking the samples out from the ovens. The results from analysis are in Appendix 1. At the initial stage, it is possible to detect portlandite, calcite, ettringite, alite and belite and calculate the amounts of them for the numerical model. In samples exposed to temperatures ettringite has decomposed which agrees to the previous studies. The intensity of portlandite peak has decreased and the intensity of calcite peak has increased as the exposure temperature has increased. There are also possibly recognised alite and belite. In both samples, the peak at the 2θ value approximately 43° may represent calcite, but it is formed only when the exposure temperature has been 345 °C. The identification of minerals from XRD-graphs is uncertain. The only certain minerals identified are portlandite and calcite, since they can also be seen from thermal analysis. Other minerals are uncertain, but for example alite and belite are possible since they are forming two different peaks. Since C-S-H-gel is amorphous, it does not form any peaks in XRD-graphs. Instead of that, it forms a "base", where other peaks rise. The change of this "base" can be observed at the low 2θ values. The identification of minerals is challenging as minerals may form peaks at the same 2θ-value and cover each other.

As with thermal analysis of samples exposed to cycles of high temperature and RH 45% or water, the XRD analysis does not show much of change in minerals. The results of SR-cement exposed to temperature and water cycles gave one divergent graph which can be due to unsuccessful analysis, since there are not such remarkable variations in thermal analysis. However, the decrease in portlandite intensity and increase in calcite intensity can be observed. Also ettringite is decomposed after temperature treatment in all the other cases, but maybe a peak can be seen at the ettringite point in samples which were in water storage after exposing to high temperatures. Al thought, as observed (Castellote et al. 2004) ettringite and C-S-H-gel does not recover after heating and water storage as portlandite and calcite.

4.2.5 Estimation of mineral fraction from thermal analysis and XRD analysis

It is possible to evaluate the amounts of portlandite and calcite from thermal analysis as their decomposition forms clear peaks in DTG-figures. Since it is also possible that some other minerals decompose at the same temperature, the calculated amounts of portlandite and calcite are the maximum amounts in cement paste. The calculation is

based on the chemical reaction of the decomposition of these minerals, which are for portlandite

$$Ca(OH)_2 \rightarrow CaO + H_2O \quad (4)$$

and for calcite

$$CaCO_3 \rightarrow CaO + CO_2 \quad (5)$$

As the same molar amount of portlandite is decomposed as water is evaporated, the amount of portlandite can be calculated from the equation

$$m(Ca(OH)_2) = \frac{M(Ca(OH)_2)}{M(H_2O)} \cdot \Delta m \quad (6)$$

where $m(Ca(OH)_2)$ is the mass percent of portlandite [%],
$M(Ca(OH)_2)$ it the molar mass of portlandite [g/mol],
$M(H_2O)$ is the molar mass of water [g/mol] and
$\Delta m$is the mass percent of water evaporated from sample in thermal analysis [%].

The original calcite amount can be calculated from the equation

$$m(CaCO_3) = \frac{M(CaCO_3)}{M(CO_2)} \cdot \Delta m \quad (7)$$

where $m(CaCO_3)$ is the mass percent of calcite [%],
$M(CaCO_3)$ is the molar mass of calcite [g/mol],
$M(H_2O)$ is the molar mass of water [g/mol] and
Δm is the mass percent of carbon dioxide evaporated from sample in thermal analysis [%].

When the portlandite amount is known, other mineral fractions can be evaluated from XRD analysis. It is possible to evaluate the amounts by comparing the relative intensities of peaks when the amount and the intensity of portlandite is known. The mineral fraction of C-S-H-gel is estimated after calculating all the other amounts and then supposing that C-S-H covers the mass remaining. According to the other studies, C-S-H decomposes before the temperature of 175 °C and that is why it is not in Table 6 and Table 7 at the temperature points of 175 °C and 345 °C. As the samples were taken

randomly from the cement paste, the values represent average amounts of minerals. In Tables 6 and 7, the calcite amount is determined from XRD and thermal analysis.

Table 6 Estimated mineral mass percents of the initial stage and after 124 d in high temperatures of OPC

Mass percent [%]	initial	95°C	175°C	345°C
Portlandite	18,18	21,35	16,07	15,47
Calcite (XRD)	3,66	4,78	5,20	7,36
Calcite (TG)	1,43	3,22	2,24	8,25
Alite	3,82	7,18	5,94	5,30
Belite	3,50	5,85	5,94	6,78
Ettringite	2,39	0,00	0,00	0,00
Hydrotalcite	1,75	0,00	0,00	0,00
Periclase	0,80	0,00	0,00	0,00
C-S-H	65,91	60,84	-	-

Table 7 Estimated mineral mass percents of the initial stage and after 124 d high temperatures of SRC

Mass percent [%]	initial	95°C	175°C	345°C
Portlandite	18,16	18,68	21,1	14,95
Calcite (XRD)	4,95	5,55	7,30	8,54
Calcite (TG)	3,23	3,5	4,36	11,1
Alite	3,56	3,77	4,24	5,98
Belite	2,63	3,37	5,89	6,83
Ettringite	2,17	0,00	0,00	0,00
Hydrotalcite	1,55	0,00	0,00	0,00
Periclase	0,77	0,00	0,00	0,00
C-S-H	66,22	68,63	-	-

5 Mathematical model for simulation

To simulate the effects of elevated temperature on cement paste, a numerical model was developed. It calculates the mineral fractions in cement paste and the related porosity as a function of time. Temperature was kept constant in calculations.

5.1 Governing equation for simulations (Steefel 2009)

The model was implemented in program GrunchFlow which is a software for modelling multicomponent reactive flow and transport developed by Carl I. Steefel, who works in Lawrence Berkeley National Laboratory as a scientist. The program uses *global implicit* or *one-step* method to solve the reaction-transport equation. This method is called GIMRT in the manual.

The governing equation for the conservation of solute mass is defined as

$$\frac{\partial}{\partial t}\left(\phi \rho_f M_{H_2O} C_i\right) + \nabla \cdot \left(-\boldsymbol{D}\nabla\left(\rho_f M_{H_2O} C_i\right) + \boldsymbol{u}\rho_f M_{H_2O} C_i\right) = R_i, \quad i = 1,2 \ldots N_{tot} \tag{8}$$

where C_i is the molar concentration of a species in solution [mol/kg of water],
M_{H2O} is the mass fraction of water [-],
ρ_f is the fluid density [kg/m^3],
u is the Darcian flux [m/s],
D is the combined dispersion-diffusion tensor [m^2/s],
R_i is the total reaction rate of species i in solution [mol/unit rock volume/unit time],
$N_{tot}$is the total number of aqueous species,
φ is the porosity [-].

The Darcian flux is related to the true velocity of the fluid, v, by multiplying it with the porosity:

$$\boldsymbol{u} = \phi \boldsymbol{v} \tag{9}$$

D is a second order tensor which is a sum of the mechanical or kinematic dispersion

coefficient $\mathbf{D}^*$ and the molecular diffusion coefficient, D_0, in water divided by the formation resistivity factor, F

$$\boldsymbol{D} = \boldsymbol{D}^* + \frac{D_0}{F} \tag{10}$$

where F is the ratio of the resistivity of the saturated porous medium over the resistivity of the pore solution alone. F is defined in the program as based on Archie's law:

$$F = \phi^{-m} \tag{11}$$

where m is cementation exponent, and the values for it are usually between 1.3-2.5.

The reaction term R_i is divided into dissolution-precipitation (heterogeneous) reactions, R_i^{min}, aqueous (homogeneous) reactions R_i^{aq}, and adsorption reactions, R_i^{ads},

$$R_i = R_i^{min} + R_i^{aq} + R_i^{ads} \tag{12}$$

The heterogeneous reaction term can be written in

$$R_i^{min} = -\sum_{m=1}^{N_m} v_{im} r_m \tag{13}$$

where r_m is the rate of precipitation or dissolution of mineral m per unit volume rock, positive as precipitation and negative as dissolution [mol/m^2/s],
v_{im} is the number of moles of i species in mineral m (or stoichiometric coefficient if the reaction is written in terms of the dissolution of one mole of the mineral) [mol],
N_m is the number of minerals present in the rock.

The first equation provides a general formulation for the conservation of solute mass, which takes no assumptions of the chemical equilibrium. However, if we assume that the various aqueous species are in chemical equilibrium, it is possible to reduce the number of concentrations that need to be solved for. This means that the total number of aqueous species N_{tot} where the number of independent chemical reactions N_c can be reduced by the number of N_x linearly independent chemical reactions between them.

This leads to division of primary, N_c or here, C_j, species and secondary N_x or X_i species. The chemical equilibrium between primary and secondary species take the form

$$A_i \rightleftharpoons \sum_{j=1}^{N_c} v_{ij} A_j \tag{14}$$

where A_i is the chemical formula of secondary species,
A_j is the chemical formula of primary species,
v_{ij} is the number of moles of primary species *j* in one mole of secondary species *i*

It should be noticed, that chemical reactions can be written in many forms and the choice between primary and secondary species is subjective. An algebraic link between the reversible reactions between the primary and secondary species is given in equation 15:

$$X_i = K_i^{-1} \gamma_i^{-1} \prod_{j=1}^{N_c} (\gamma_j C_j)^{v_{ij}}, \quad i = 1, \dots N_x \tag{15}$$

where γ_i is the activity coefficient of secondary species [-],
γ_j is the activity coefficient of primary species [-],
K_i is the equilibrium constant of the chemical reaction of equation (14) [-].

Equation (14) implies that the rate of production of a primary component *j* due to homogenous reactions can be written in terms of the sum of the total rates of production of the secondary species

$$R_j^{aq} = -\sum_{i=1}^{N_x} v_{ij} r_i \tag{16}$$

where r_i are the reaction rates of the secondary species [mol/m^2/s].

The equation can be understood that during the dissolving of minerals, they only produce primary species which then equilibrate instantly with the secondary species in the system.

The term R_j^{min} is the only one to stay on right hand side of the original reaction (equation 12) since it is the only kinetic reaction. The original equation has the form:

$$\frac{\partial}{\partial t}\left(\phi\rho_f M_{H_2O}\left(C_j + \sum_{i=1}^{N_x} v_{ij}X_i\right)\right) + \nabla \cdot \left(-\boldsymbol{D}\nabla\left(\rho_f M_{H_2O}\left(C_j + \sum_{i=1}^{N_x} v_{ij}X_i\right)\right) + \boldsymbol{u}\rho_f M_{H_2O}\left(C_j + \sum_{i=1}^{N_x} v_{ij}X_i\right)\right) = R_j^{min}, \quad i = 1,2 \dots N_{tot} \tag{17}$$

When the total concentration U_j is defined as

$$U_j = C_j + \sum_{i=1}^{N_x} v_{ij}X_i \tag{18}$$

the governing differential equations can be written in terms of total concentrations in the case were only aqueous (mobile) species are involved.

$$\frac{\partial}{\partial t}\left(\phi\rho_f M_{H_2O}U_j\right) + \nabla \cdot \left(-\boldsymbol{D}\nabla\left(\rho_f M_{H_2O}U_j\right) + \boldsymbol{u}\rho_f M_{H_2O}U_j\right) = R_j^{min}, \quad i = 1,2 \dots N_{tot} \tag{19}$$

The equilibrium constants for reactions are given in database for temperatures 25 °C – 300 °C at pressures corresponding to the water saturation curve. A temperature dependence is also included in the reaction rate constants, diffusion coefficients and fluid viscosities. The rate constant at other temperatures than 25 °C can be calculated from Arrhenius equation:

$$k = k_{25}\exp\left(\frac{-E_a}{R}\left(\frac{1}{T} - \frac{1}{295{,}15}\right)\right) \tag{20}$$

where k_{25} is the reaction rate constant at 25 °C,

E_a is the activation energy [J/mol],

R is the gas constant, 8,314 [J/(Kmol)],

T is the temperature [K].

The program uses the extended Debye-Hückel formulation to calculate the activity coefficients for the ionic species. The Debye-Hückel equation is given by

$$log\gamma_i = -\frac{Az_i^2(I)^{\frac{1}{2}}}{1 + Ba_i(I)^{\frac{1}{2}}} + b_i I \tag{21}$$

where A [-] and B [-] are the temperature-dependent coefficients,

a_i [-] and b_i [-] are the ion-specific fitting parameters.

The ionic strength *I* of the solution can be written as

$$I = 0.5\sum_{i=1}^{n} z_i^2 c_i \tag{22}$$

where z_i is the charge number of ionic species i in solution and

n is the total number of ionic species i in aqueous solution.

The coefficients for the temperature dependence are taken from the EQ3 database.

5.2 Program structure

The steps in calculation are represented in Figure 19. At first, the program specifies the initial and boundary conditions which user has determined. After that, it starts stepping through time. On each time step, a series of Newton iterations is applied to calculate the f_j:s, the discretized differential equations for the total concentration of each primary species. The terms $\partial f_j/\partial C_j$ create the Jacobian submatrices and form the global Jacobian matrix **A**. If f_j are defined to make the elements of vector **b**, the equation for solving the change of primary species gets the form:

$$\mathbf{A} \cdot \boldsymbol{\delta}\mathbf{C} = \mathbf{b} \tag{23}$$

Once δC_j are computed, they are used to update the total concentrations of the primary species

$$C_j^{new} = C_j^{old} + \delta C_j \tag{24}$$

This completes the Newton iteration. Convergence is achieved when the f_j:s are reduced to a tolerance set in the code (in this, $f_j \approx 0$). Once convergence is achieved, program updates the mineral properties. The individual mineral fractions are calculated with equation:

$$\phi_m(t + \Delta t) = \phi_m(t) + V_m r_m(t + \Delta t)\Delta t \tag{25}$$

where V_m is the molar volume and r_m is the reaction rate of mineral. The porosity is calculated from mineral fractions

$$\phi = 1 - \sum_{k=1}^{N_m} \phi_m \tag{26}$$

Both mineral volume fractions and reactive surface areas are assumed to be constant during one time step. The reactive surface areas are updated according to equations:

$$A_m = A_{m,0} \begin{cases} \left[\left(\frac{\phi}{\phi_0}\right)\left(\frac{\phi_m}{\phi_{m,0}}\right)\right]^{2/3} & dissolution \\ \left[\frac{\phi}{\phi_0}\right]^{2/3} & precipitation \end{cases} \tag{27}$$

for primary minerals (initially present in calculations), and for secondary minerals (possibly forming minerals):

$$A_m = A_{m,0} \begin{cases} \left[\left(\frac{\phi}{\phi_0}\right)\phi_m\right]^{2/3} & dissolution \\ \left[\frac{\phi}{\phi_0}\right]^{2/3} & precipitation \end{cases} \tag{28}$$

where $\phi_{m,0}$ is the initial volume fraction of mineral m and ϕ_0 is the initial porosity, $A_{m,0}$ is the initial reactive surface area [m^2/m^3]. The default reactive surface area for all minerals in program is 100 m^2/m^3. (Steefel 2009)

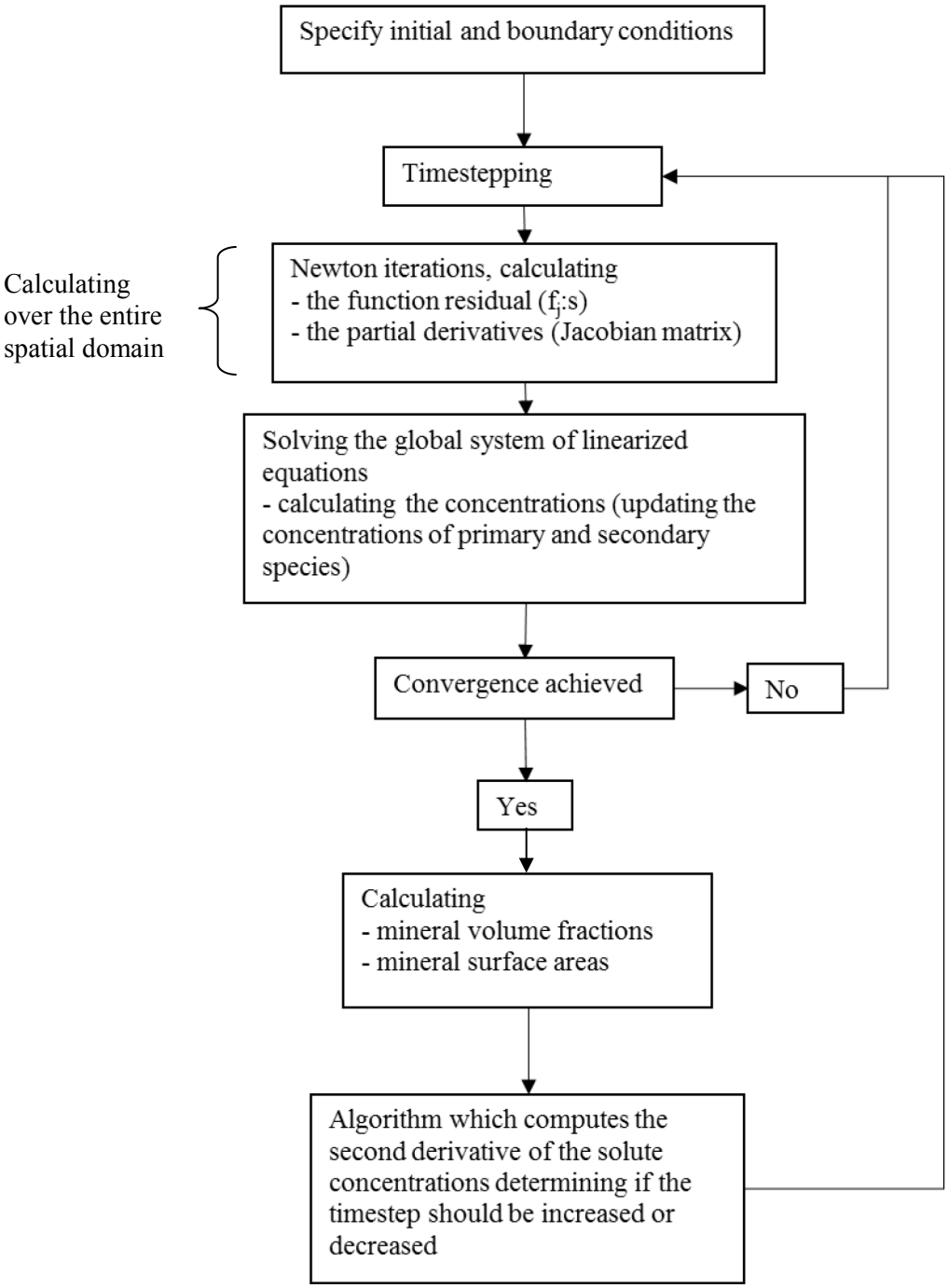

Figure 19 The program structure of CrunchFlow (Steefel 2009)

Maximum time step was one day. The grid consists of twenty cells, with equal length. As all the reactions were expected to be happen at the surface of sample, a short grid with 20 cells was chosen. The saturation was fixed to 0.45 during the whole calculation time. The model was one-dimensional.

Tables 8-10 presents the parameters needed for calculations. The initial amounts of mineral have been determined experimentally and pore solution was taken from the study of Kari et al. 2013. Diffusion coefficients are in

Table 9 and mineral properties in Table 10. Both of them are taken from literature (Mills et al. 1989, Fernandez et al. 2010).

Table 8 The initial conditions of sulphate resisting and ordinary portland cement used in calculations

Initial conditions	OPC [V-%]	SR-cement [V-%]	Pore solution [mmol/l] (Kari et al. 2013)
Portlandite	12,36	12,35	
Calcite	2,06	2,78	
C-S-H	43,4	43,53	
Periclase	0,34	0,33	
Ettringite	2,06	1,87	
Hydrotalcite	1,36	1,2	
OH^-			235
Ca^{2+}			1,8
K^+			234,54
$SO4^{2-}$			25,88
Na^+			44,8
Mg^{2+}			0,12
SiO_2(aq)			1,1
AlO_2^-			0,22
Fe^{3+}			0,32
Porosity [-]	0,35	0,35	
Tortuosity (Kari et al. 2013)	0,038	0,038	

Table 9 Diffusion coefficients of aqueous species (Mills et al. 1989)

Diffusion coefficient [10^{-5} cm^2/s]	25 °C	95 °C	175 °C	345 °C
H^+	9,6	20,0	30,7	53,5
Na^+	1,4	5,4	12,0	26,1
K^+	1,8	6,2	13,2	28,2
Ca^{2+}	0,9	3,7	8,0	17,3
AlO_2^-				
Mg^{2+}	0,7	1,7	2,8	5,2
OH^-	5,5	14,4	24,8	46,8
SiO_2				
$SO4^{2-}$	1,2	2,7	4,5	8,6

HCO_3^-	1,19	1,19	1,19	1,19
CO_2(gas)	3,45	3,45	3,45	3,45

Table 10 Mineral properties (Fernandez et al. 2010)

Mineral	Reaction rate (T=25 °C) (logarithm value)	Activation energy [kcal/mol]	Reactive surface area [m^2 solid phase/m^3 porous media]	Molar volume [cm^3/mol]	Molar mass [g/mol]
Calcite $CaCO_3$	-6,0	8,46	100	39,934	100,0872
Ettringite $Ca_6Al_2(SO_4)_3(OH)_{12}:26H_2O$	-8,0	10	100	710,32	1255,1072
C-S-H(1,6) $Ca_{1.6}SiO_{3.6}:2.58H_2O$	-7	10	100	84,68	196,2876
Portlandite $Ca(OH)_2$	-8	10	100	33,056	74,0927
Brucite $Mg(OH)_2$	-6	14,34	100	24,63	58,3197
Periclase MgO	-8,0	15,0	100	11,248	40,3044
Dicalcium silicate Ca_2SiO_4	-12,0	15,0	100	59,11	172,2391

In Figure 20, the calculation model with its boundary conditions is represented. Grid represents the cement paste consisting of minerals and pore solution and the boundary conditions. Temperature and the degree of saturation are constant over the grid.

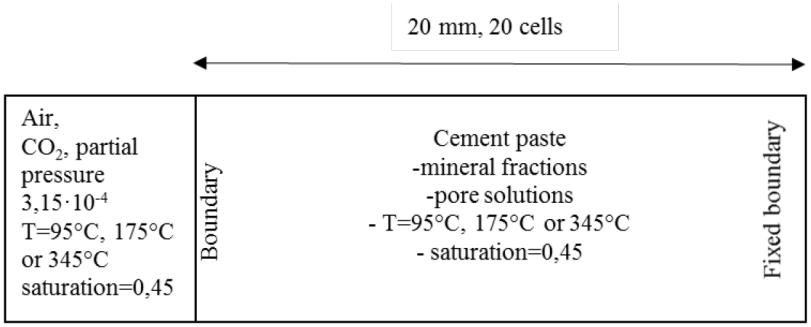

Figure 20 Schematic figure of the calculated situation

5.3 Results from simulation and their comparison to experimental results

In Figures 21-26, the results of the simulations performed and their comparison to the experimental results are represented. Portlandite and calcite amounts were chosen to closer examination since those amounts are the most certainly determined by XRD and thermal analysis. In all of these figures, lines presents the calculated values and dots presents the experimental values. In the calculations, the trends of the profiles are caused by the boundary conditions at the surface subjected to air. Carbon dioxide is affecting mainly the mineral amounts there. When comparing the calculations and experimental results, it can be seen that the match is better for temperature of 175 °C and 345 °C.

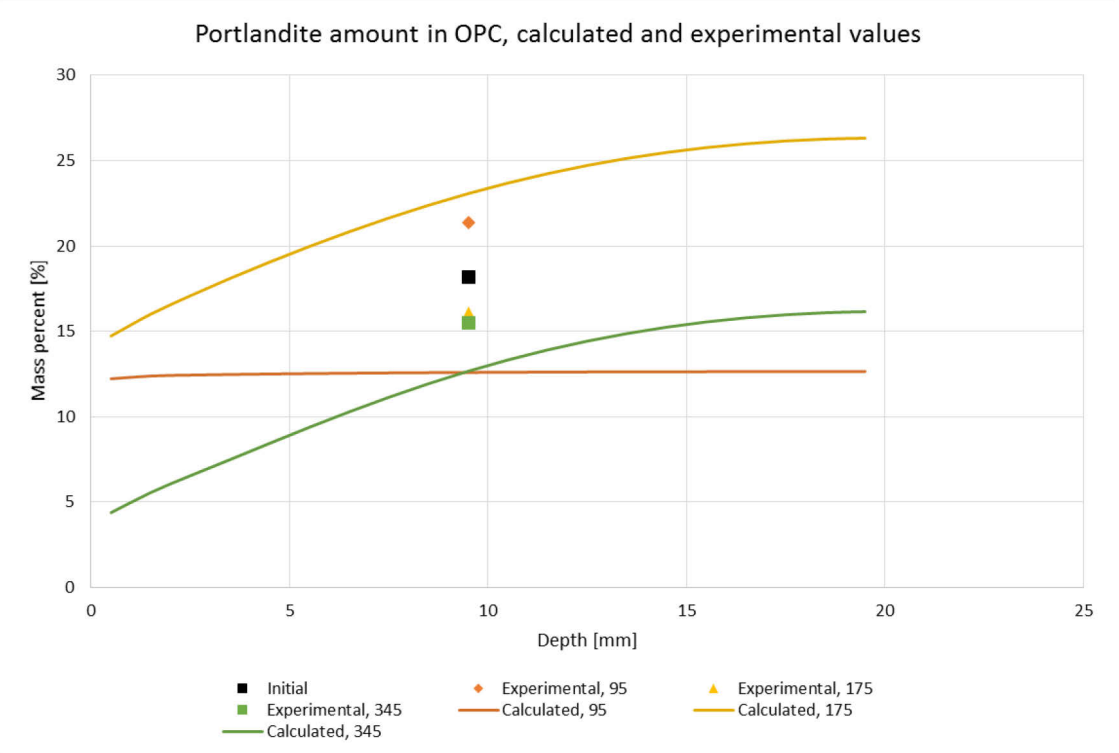

Figure 21 Calculated and experimental values for portlandite amount in OPC at the initial stage and after 124 d in temperatures of 95 °C, 175 °C and 345 °C

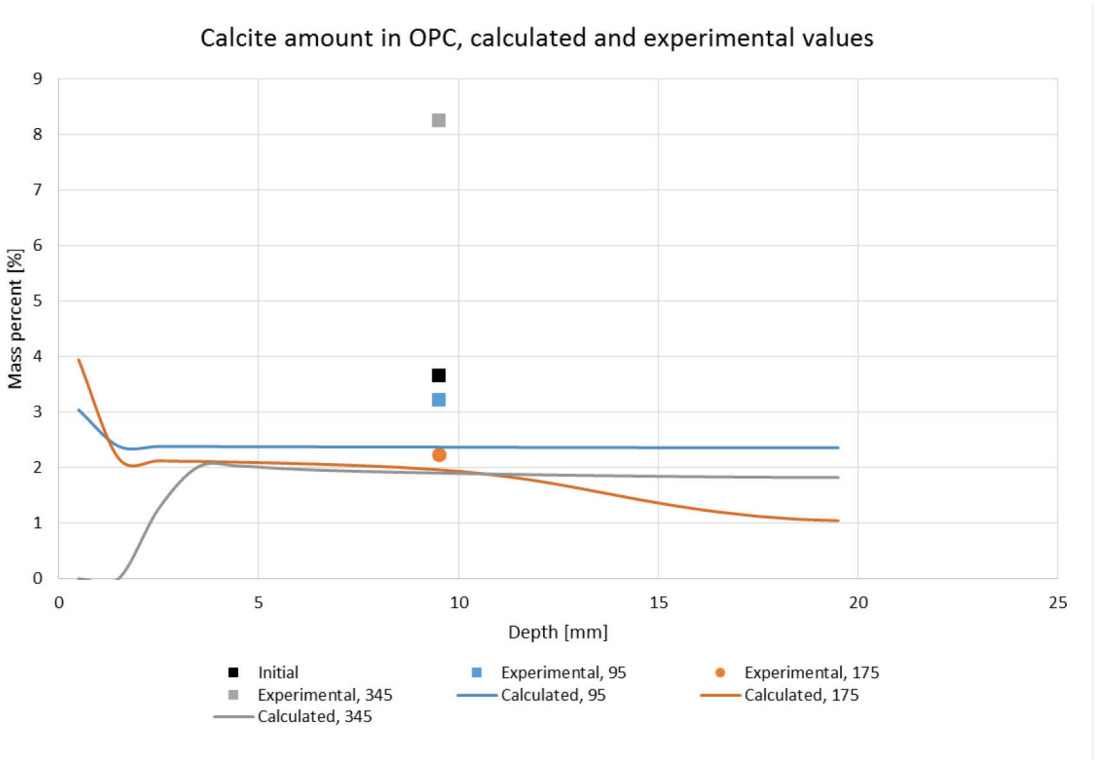

Figure 22 Calculated and experimental values for calcite amount in OPC at the initial stage and after 124 d in temperatures of 95 °C, 175 °C and 345 °C

When the calculation temperatures has been 95 °C, portlandite amount has decreased in both cements, which is not the case according to the experiments as the measured values are larger than initially. It is possible that the increase in experimental values is due to proceeding hydration. At the temperature of 175 °C, portlandite amount has increased according to calculations and the measured value for SR-cement is also larger than initially. However, the measured value for OPC is smaller than initially, but calculated and experimental values are in accordance.

Calcite amounts of cements at the temperatures of 95 °C and 175 °C are more like in experiments than at the temperature of 345 °C. The amounts of calcite measured from samples in Figures 22 and 24 are according to the thermal analysis.

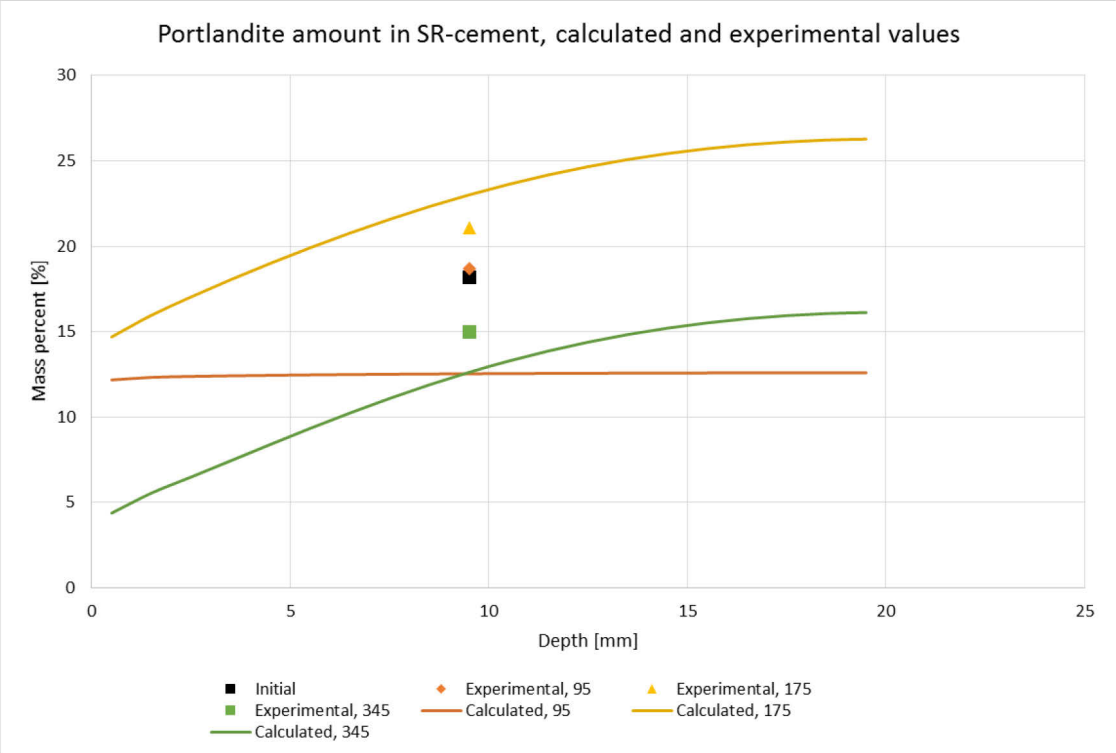

Figure 23 Calculated and experimental values for portlandite amount in SR-cement at the initial stage and after 124 d in temperatures of 95 °C, 175 °C and 345 °C

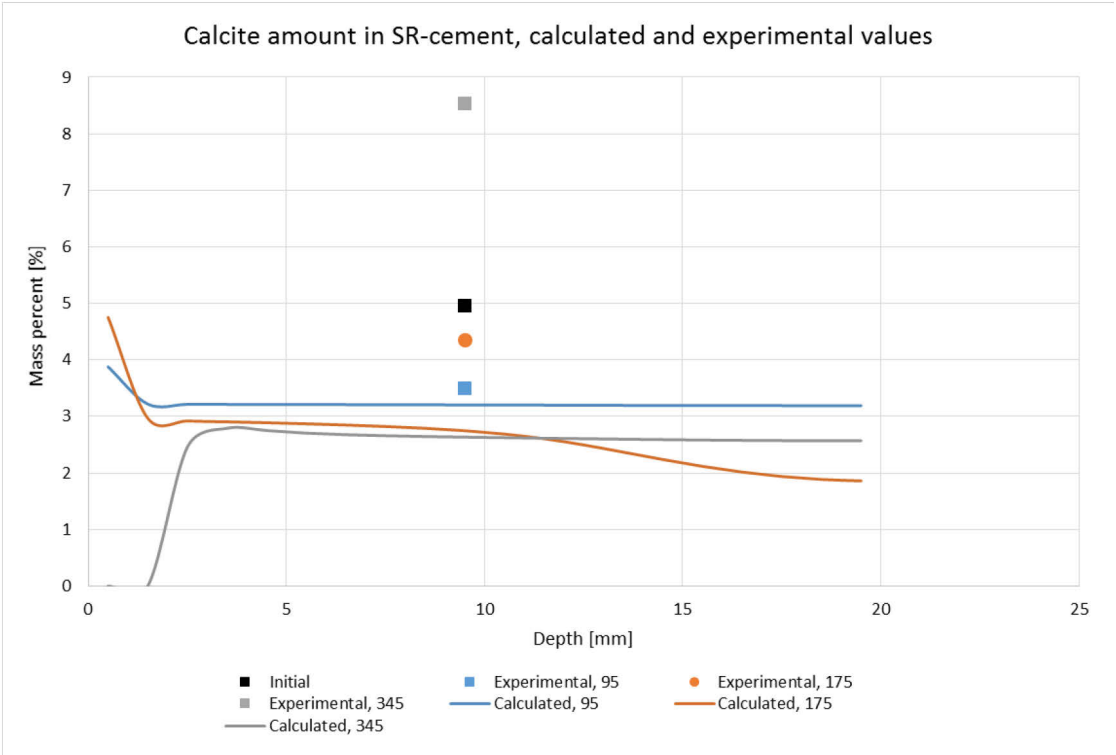

Figure 24 Calculated and experimental values for calcite amount in SR-cement at the initial stage and after 124 d in temperatures of 95 °C, 175 °C and 345 °C

When comparing porosity results, in all cases (calculated and measured) porosity has increased as temperature has increased which is in accordance with the theory. Calculated values for porosity at the temperatures 175 °C and 345 °C are larger than experimentally determined for both cases but the values are quite similar.

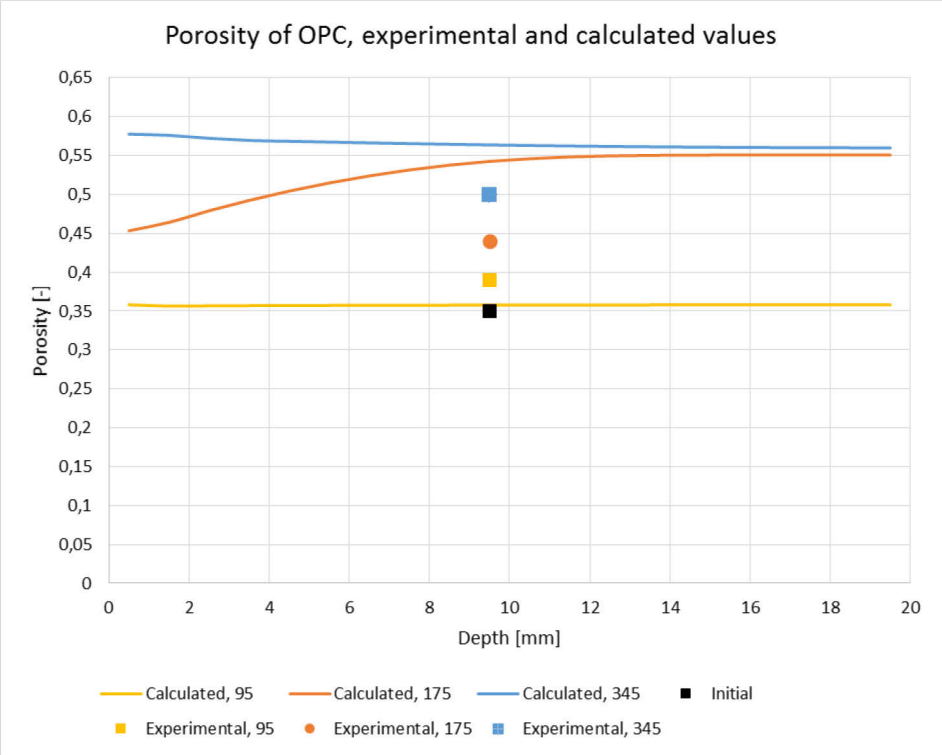

Figure 25 Calculated and experimental values for porosity of OPC at the initial stage and after 124 d in temperatures of 95 °C, 175 °C and 345 °C

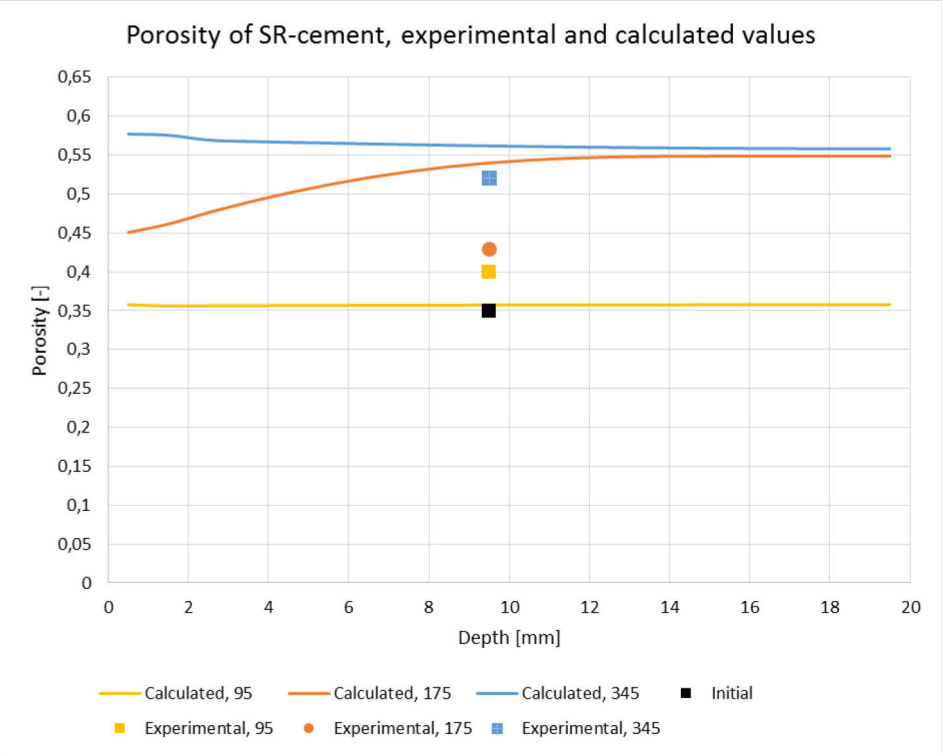

Figure 26 Calculated and experimental values for porosity of SR-cement at the initial stage and after 124 d in temperatures of 95 °C, 175 °C and 345 °C

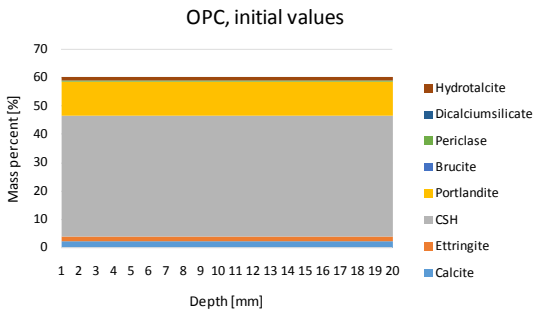

Figure 27 a

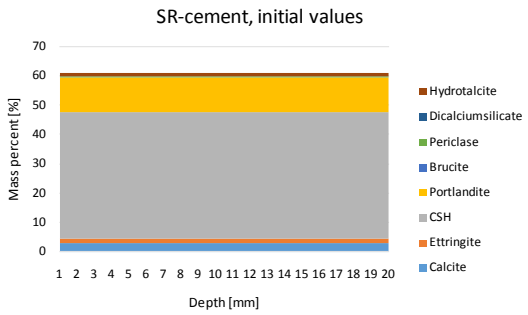

Figure 27 b

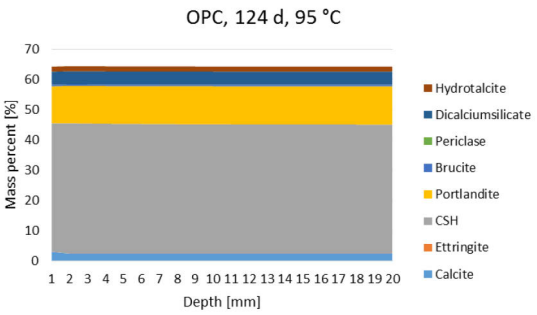

Figure 27 c

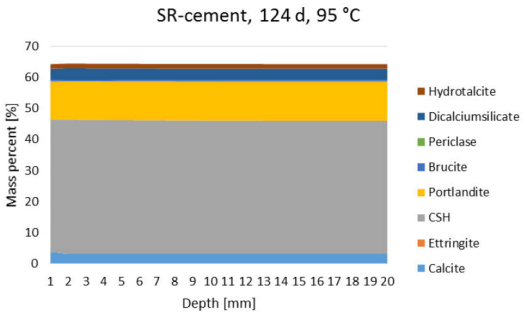

Figure 27 d

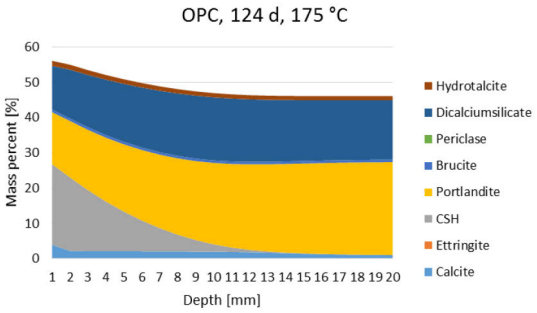

Figure 27 e

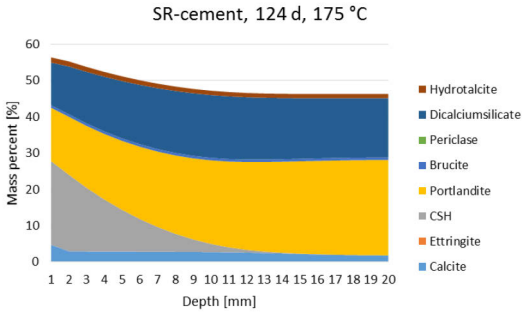

Figure 27 f

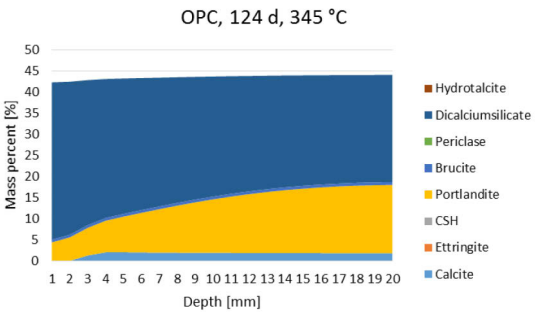

Figure 27 g

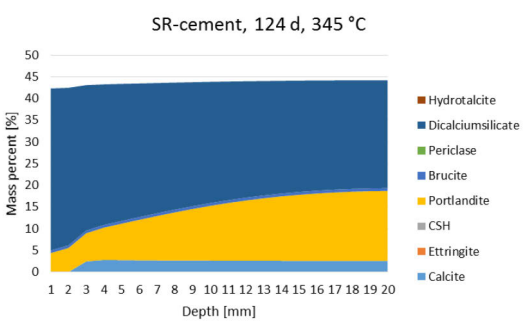

Figure 27 h

Figure 27 a, b, c, d, e, f, g, h Initial and calculated mineral mass fractions after 124 d in high temperatures of OPC and SR-cement. The white area represents the porosity of cement paste.

In Figure 27 a-h, are given the calculated mineral mass fractions. It can be seen that when the temperature is 95 °C, the main compound is C-S-H and the second largest mass percent is that of portlandite. Ettringite has decomposed. Dicalciumsilicate amount, which presents the both alite and belite amount, is almost the same as initially. As the temperature is higher, more dicalciumsilicate is composed. This is due to the decomposition of C-S-H. When the temperature is 175 °C, the main compound is portlandite, and C-S-H is still present at the boundary and there is less dicalciumsilicate than further depth. When the temperature is 345 °C, more dicalciumsilicate is composed since C-S-H has decomposed. Also portlandite and calcite are still left in cement pastes. Porosity can also be determined from Figures based on the empty space related to change of mass fractions. It can be noticed that porosity is related to the amounts of calcite and C-S-H and is increasing as calcite or C-S-H amount decrease.

5.4 Long-term simulations

Calculations were also made for longer period to evaluate the long-term effects of high temperature on cement paste. Figures 28 and 29, the results from calculations after one and two years of exposure are represented. As a comparison, also the results after 124 d are presented again. When temperature is 95 °C, significant changes have not happened, when comparing to the results at 124 d. Only minor formation of calcite caused by carbonation can be seen near the surface. If the temperature is 175 °C, C-S-H has almost disappeared after one year and completely after two years. There can also be seen the carbonation taken place near the boundary. Dicalciumsilicate has formed as C-S-H has decomposed. When the temperature is 345 °C, dicalciumsilicate is the main compound according to the calculations. Some calcite is still left, but almost all portlandite has decomposed.

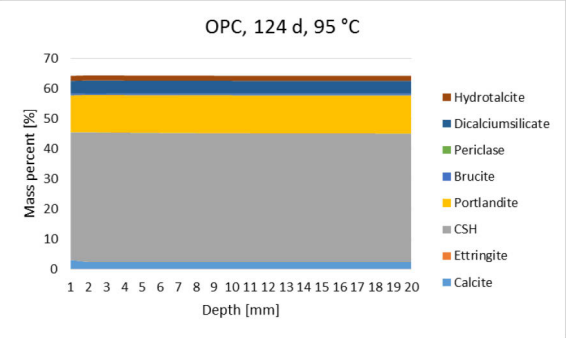

Figure 28 a

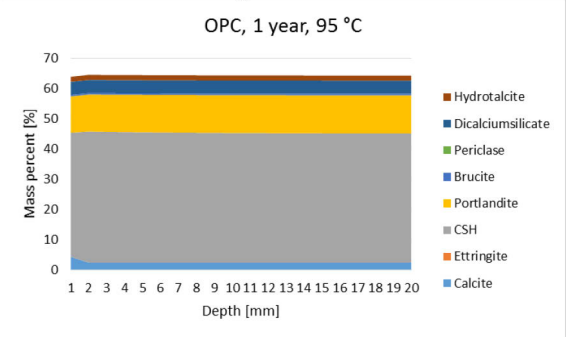

Figure 28 b

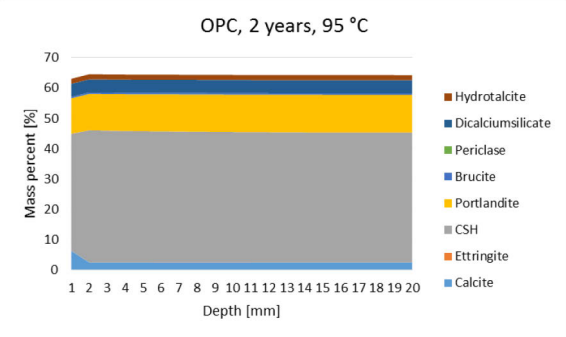

Figure 28 c

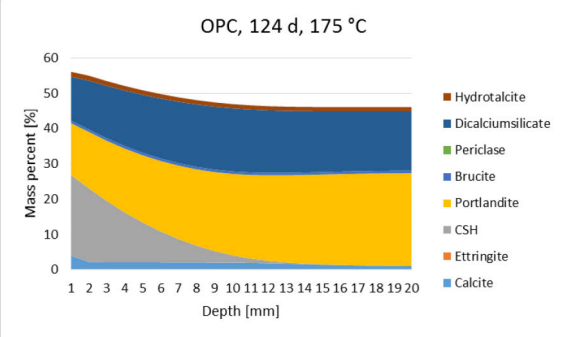

Figure 28 d

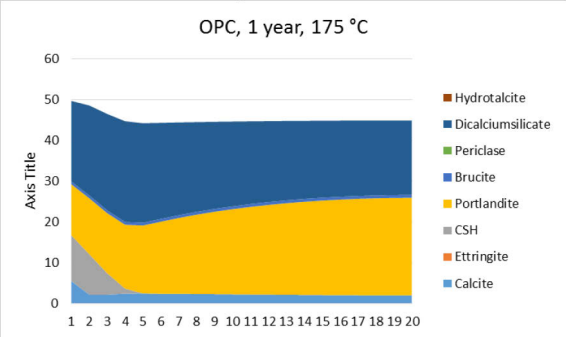

Figure 28 e

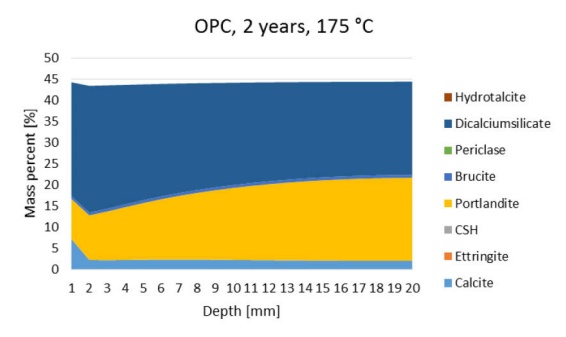

Figure 28 f

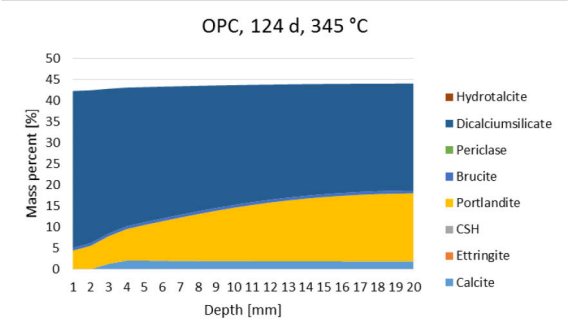

Figure 28 g

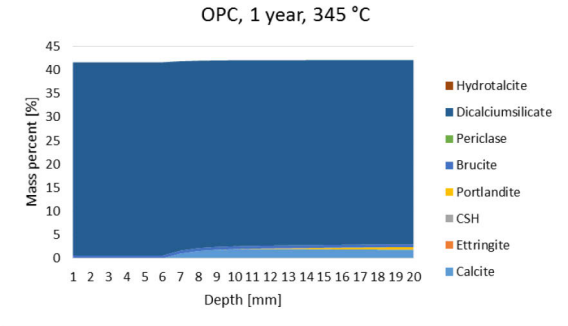

Figure 28 h

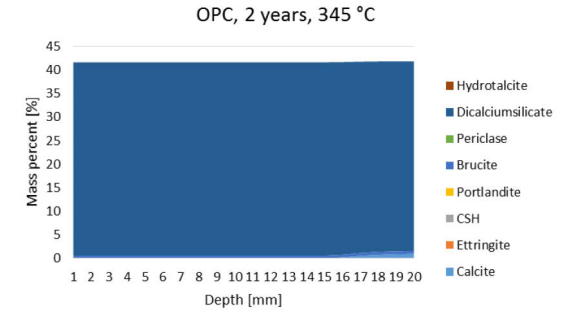

Figure 28 i

Figure 28 Calculated mineral mass fractions after one and two years in high temperatures. The white area represents the porosity of cement paste.

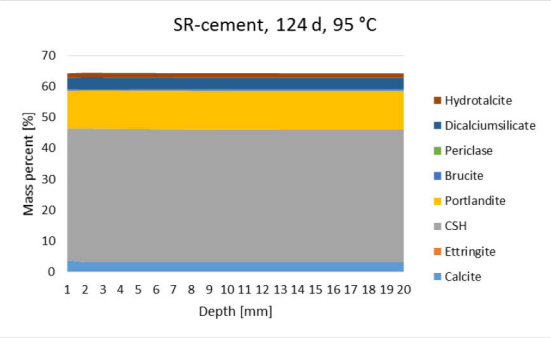

Figure 29 a

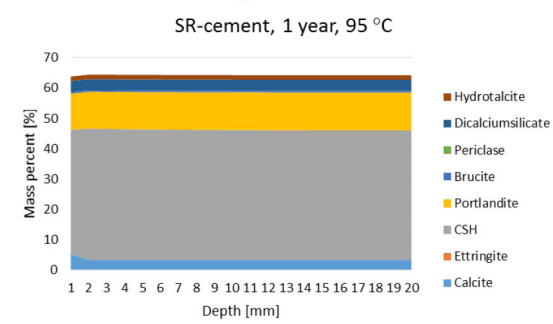

Figure 29 b

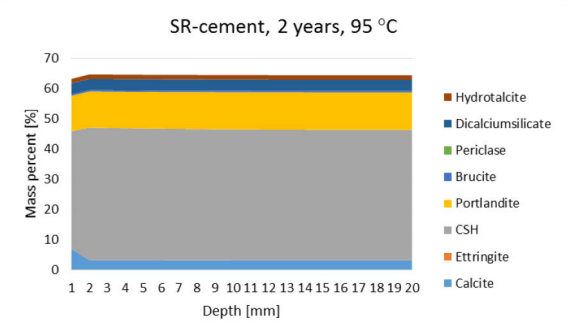

Figure 29 c

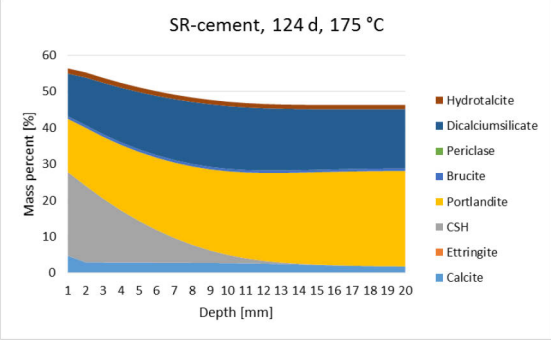

Figure 29 d

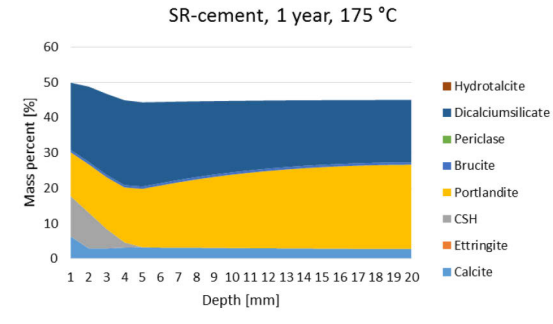

Figure 29 e

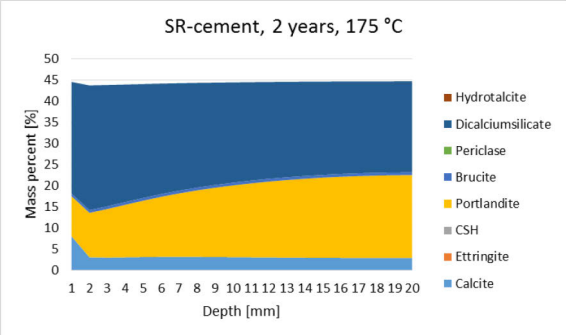

Figure 29 f

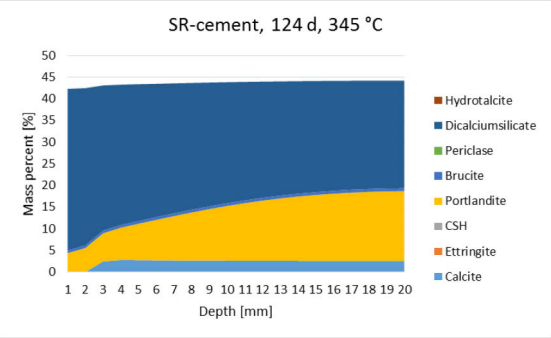

Figure 29 g

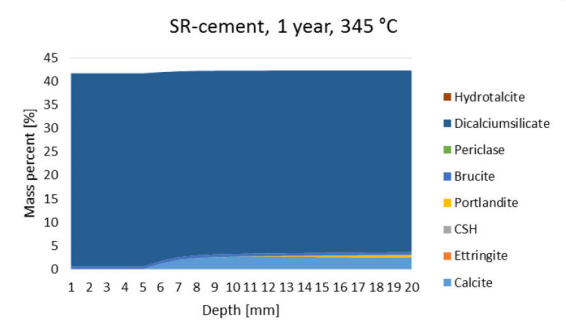

Figure 29 h

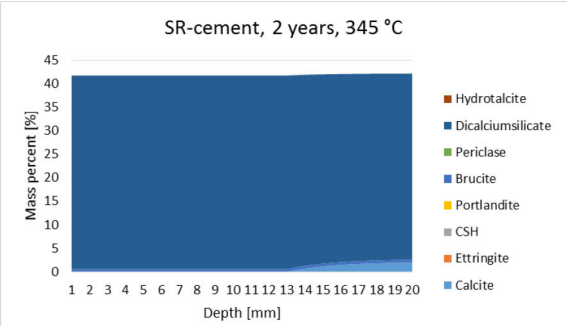

Figure 29 i

Figure 29 Calculated mineral mass fractions after one and two years in high temperature. The white are represents the porosity of cement paste

The calculated porosities of cement paste after one and two years in high temperatures are given in Figure 30. The increase of porosity is higher at the temperatures of 175 °C and 345 °C than at 95 °C, where the porosity increase is not significant as the initial porosity was 0,35 for both cements. When considering porosity only, the temperatures 175 °C and 345 °C does not lead to differences results in long time simulations. In both cases, C-S-H is almost or completely disappeared and that affects the porosity.

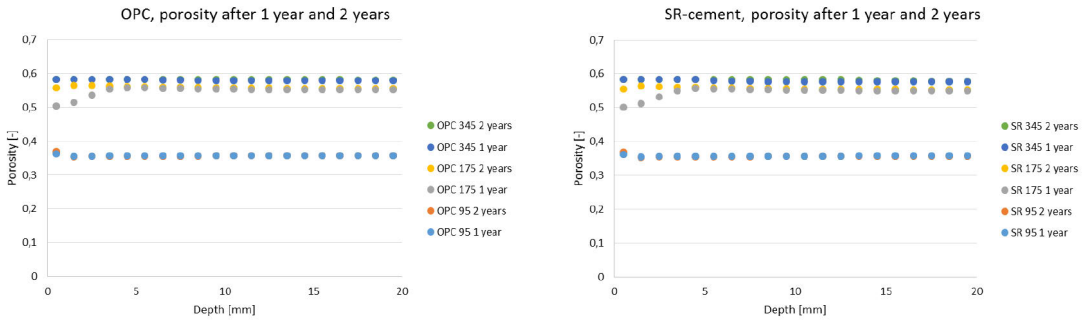

Figure 30 Porosities after one and two years in high temperatures

6 Analysis of uncertainty

The experimental studies were done only for the cement paste, not for the concrete. This was chosen to separate the phenomena studied from aggregates, which would disturb the methods used in experimental program. However, cement paste does not fully correspond concrete and, for example, the effect of ITZ area on the deteriorations not taken into account as studying only cement paste. The movement of moisture and the saturation states of cement paste samples at different temperatures were not studied experimentally, and the values were taken from the literature, which might include a potential source of error. To reduce the uncertainty of experimental work, more samples for each case would be recommended. This would also increase the certainty of simulations.

The porosity test used in this study does not separate different kinds of pores (capillary and gel). It only represents the total porosity. However, as the meaning of porosity test was to provide information of the quality and performance of cement paste at the initial stage and after temperature treatment, it was not so important to separate different kinds of pores. As comparing the experimental and simulations results, total porosity was applied since the simulation model calculates the total porosity. Because of the complexity of the test, the pore solutions of these cement pastes were not determined experimentally. However, the values determined previously for same cement quality and same water-to-cement ratio were used for both cement types, which may have a minor effect on the results.

The choice of reaction rates and mineral surface areas had to be done for simulations, logK-values were found from database. It was found that the value of reaction rate affects quite much on the results. To determine the reaction rate experimentally is quite a challenge and no consensus for absolute values exists generally. The values were taken from other study, but obviously, this is a possible source of uncertainty in the simulations, since case-specific values were not available.

In the simulations, movement of moisture due to temperature changes was not taken into account. However, defining the saturation conditions was challenging and, as a matter of fact the saturation was fixed to a certain value for the whole calculation time.

Even though the modeling included some sources of uncertainties, the results are based on chemical constants of the minerals and the results reliably pointed out that elevated temperatures clearly affect cement paste and concrete.

7 Conclusions

Possible deterioration mechanisms of concrete and cement paste due to elevated temperatures were studied. According to the existing literature, deterioration of cement paste or concrete is connected to the water content and mineral properties. Change of porosity caused by elevated temperature is resulting from both of these: as water evaporates, the porosity increases which is also the result of decomposition of cement hydrates. Delayed ettringite formation was found not to be an issue for deterioration in this study under long term exposure to high temperatures. Even in samples, held in water storage after a long time at high temperatures, expansion caused by ettringite would be very unlikely according to the literature review. Relevant mechanism on cement paste ageing due to long time exposure in elevated temperature are dehydration and related porosity increase, water movement, possibly spalling, carbonation and drying shrinkage.

A numerical model for studying the effects of elevated temperature on cement paste ageing was proposed in this study. The model was based on reaction rates, logK-values and mineral surface areas and other properties such as molar mass and volume. The results were compared with the values received experimentally. The simulations suggested, that temperature of 95 °C is not very severe for cement paste, but when temperature is 175 and exposure long enough (1-2 years) the main hydration product of cement paste, C-S-H, is decomposed and this clearly affects the structure of paste. C-S-H forms continuous structure on hardened cement paste and engineering properties of concrete are related to C-S-H. As the C-S-H is lost, also the structural resistance of concrete may be lost. According to the experimental results, ordinary portland cement has better resistance against the effects high temperature since after exposing to high temperature its compressive strength was higher and porosity was smaller than those of SR-cement. These changes were hard to see from calculations since the amounts of minerals at the initial stage were so similar.

In experiments only one water-to-cement ratio was chosen. In the future, it would be interesting in studying the effect of water-to-cement ratio on the ageing of cement paste or concrete exposed to the elevated temperature. Also different types of cements and cements with supplementary binding materials should be studied. A series of

experimental results would be needed for studying the effects of elevated temperature on concrete or cement paste statistically. This would also make it possible to quantify the uncertainty of modelling, which is needed for implementing the model in practical engineering.

8 References

Alonso, C., Fernandez, L. Dehydration and rehydration processes of cement paste exposed to high temperature environments. Journal of Material Science, 2004. Vol 39:9. P. 3015-3024.

ASME Sec III Division 2, Code for concrete containments. Rules for construction of nuclear facility components

Aydin, S., Baradan, B. Effect of pumice and fly ash incorporation on high temperature resistance of cement based mortars. Cement and Concrete Research, 2007. Vol 37:6. P. 988-995.

Baur, I., Keller, P., Mavrocordatos, D., Wehrli, B., Johnson, C. A. Dissolution-precipitation behaviour of ettringite, monosulphate and calcium silicate hydrate. Cement and Concrete Research, 2004. Vol 34:2. P. 341-348.

Bertolinen, L., Elsener, B., Pedeferri, P., Polder, R. Corrosion of Steel in Concrete. WILEY-VCH Verlag GmbH & Co. KGaA, Weinhem. 2004. 392 p. ISBN 3-527-30800-8

Brown, P.W in Course CIV1299S, May 17-21, 2010, University of Toronto, Department of Civil Engineering. 2010.

Brunetaud, X., Linder, R., Divet, L., Duragrin, D., Damidot, D. Effects of curing conditions and concrete mix design on the expansion generated by delayed ettringite formation. Materials and Structures, 2007. Vol 40:6. P. 567-578.

Castellote, M., Alonso, C., Andrade, C., Turrillas, X., Campo, J. Composition and microstructural changes of cement pastes upon heating as studied by neutron diffraction. Cement and Concrete Research, 2004. Vol 34:9. P. 1633-1644.

Chen, J. J., Thomas, J. J., Taylor, H. F. W., Jennigs, H. M. Solubility and structure of calcium silicate hydrate. Cement and Concrete Research, 2004. Vol 34:9. P. 1499-1519.

Collepardi, M. A state-of-the-art review on delayed ettringite formation attack on concrete. Cement and Concrete Composites, 2003. Vol 25:4-5. P. 401-407.

Diamond, S. Delayed ettringite formation – Processes and problems. Cement and Concrete Composites, 1996. Vol 18:3. P. 205-215.

England, G. L., Khoylou, N. Moisture flow in concrete under steady state non-uniform temperature states: experimental observation and theoretical modeling, Nuclear Engineering and Design, 1995. Vol 156:1-2. P. 83-107.

Famy, C., Scrivener, K. L., Atkinson, A., Brough, A.R. Influence of the storage condition on the dimensional changes of the heat-cured mortars. Cement and Concrete Research, 2001. Vol 31:5. P. 795-803.

Farage, M. C. R., Sercombe, J., Gallé C. Rehydration and microstructure of cement paste after heating at temperatures up to 300 °C. Cement and Concrete Research, 2003. Vol 33:7. P. 1047-1056.

Fernandez, R., Cuevas, J., Mäder, U. K. Modeling experimental results of diffusion of alkaline solutions through a compacted bentonite barrier. Cement and Concrete Research, 2010. Vol 40:8. P. 1255-1264.

Fu, Y., Beaudoin J.J. Microcracks as a precursor to delayed ettringite formation in cement systems. Cement and Concrete Research, 1996. Vol 26:10. P. 1493-1498.

Georgali, B., Tsakiridis, P. E. Microstructure of fire-damaged concrete. A case study. Cement & Concrete Composites, 2005. Vol 27:2. P. 255-259.

Handoo, S. K., Agarwal, S., Agarwal, S.K. Physicochemical, mineralogical, and morphological characteristics of concrete exposed to elevated temperature. Cement and Concrete Research, 2002. Vol 32:7. P. 1009-1018.

Ichikawa, Y., England, G. L. Prediction of moisture migration and pore pressure build-up in concrete at high temperatures. Nuclear Engineering and Design, 2004. Vol 228:1-3. P. 245-259.

iti.northwestern.edu/cement, 29.11.2013

Janotka, I., Nürnbergerová, T. Effect of temperature on structural quality of the cement paste and high-strength concrete with silica fume. Nuclear Engineering and Design, 2005. Vol 235:17-19. P. 2019-2032.

Jennings, H. M. A model for the microstructure of calcium silicate hydrate in cement paste. Cement and Concrete Research, 2000. Vol 30:1. P. 101-116.

Jernejcic, J., Vene, N., Zajc, A. Thermal decomposition of α-dicalcium silicate hydrate. ThermochimicaActa, 1977. Vol 20:2. P. 237-247.

Kalifa, P., Menneteau, F-D., Quenard, D. Spalling and pore pressure in HPC at high temperatures. Cement and Concrete Research, 2000. Vol 31:12. P. 1915-1927.

Kari, O-P. Modelling the Durability of Concrete for Nuclear Waste Disposal Facilities. Licentiate Thesis. Teknillinenkorkeakoulu. Espoo. 2009. 101 p.

Kari, O-P., Elaknerwaran, Y., Nawa, T., Puttonen, J. A model for a long-term diffusion of multispecies in concrete based on ion-cement-hydrate interaction. Journal of Materials Science, 2013. Vol 48:12. P. 4243-4259.

Kasami, H., Hironobu, N., Tamura, M., Ichihara, Y., Maenaka, T. Evaluation of temperature, moisture evaporation and strenght of concrete subjected to sustainde elevated temperatures up to 300 °C. Transactions, SMiRT-22, 2013.

Kelham, S. The Effect of Cement Composition and Fineness on Expansion Associated with Delayed Ettringite Formation. Cement & Concrete Composites, 1996. Vol 18:3. P. 171-179.

Khan, M. I., A novel method for measuring porosity of high strength concrete. Proceedings of the 7th Saudi Engineering Conference (SEC7)

Komonen, J., Penttala, V. Effects of high temperature on the pore structure and strength of plain an polypropylene fiber reinforced cement pastes. Fire Technology, 2003. Vol 39:1. P. 23-34.

Kontani, O., Ichikawa, Y., Ishizawa, A., Takizawa, M., Sato, O., Irradiation Effects on Concrete Structure, International Symposium on the Ageing Management of Nuclear Power Plants, 2010. P. 173-182.

Lagerblad, B., Trägårdh, J. Conceptual model for concrete long time degradation in deep nuclear waste repository. Swedish Cement and Concrete Research institute, 1994. SKB Technical Report 95-21.

Lawrence, C. D. Mortar expansion due to delayed ettringite formation. Effects of curing period and temperature. Cement and Concrete Research, 1995. Vol 25:4. P. 903-914.

Lion, M., Skoczylas, F., Lafhaj, Z., Sersar, M. Experimental study on a mortar. Temperature effects on porosity and permeability. Residual properties or direct measurements under temperature. Cement and Concrete Research, 2005. Vol 36:10. P. 1937-1942.

Ljungkrantz, C., Möller, G., Peterson, N. Betonghandbok. AB Svenks Byggtjänst och Cementa AB. 1994. 1127 p.

Maekawa, K., Ishida., T., Kishi, T. Multi-scale modeling of structural concrete. 1st edition. Oxon, United Kingdom: Taylor & Francis. 655 p. ISBN 0-415-65554-0

Matsuzawa, K., Kitsutaka, Y., Tsukagoshi, M. Effect of humidity on Rate of carbonation of concrete exposed to high-temperature environment. International Symposium on the Ageing Management of Nuclear Power Plants, 2010. P. 109-114.

Menéndez, E., Andrade, C. Study of dehydration and rehydration of portlandite in mature and young cement pastes Journal of Thermal Analysis and Calorimetry, 2012. Vol 110:1. P. 443-450.

Mills, R., Lobo, V. M. M. Self-diffusion in electrolyte solutions. Physical Sciences Data 36, 1989.

Naus, D., J. A Compilation of elevated temperature concrete material property data and information for use in assessments of nuclear power plant reinforced concrete structures. United States Nuclear Regulatory Commission, 2010.

Odler, I., Chen, Y. Effect of cement composition on the expansion of heat-cured cement pastes. Cement and Concrete Research, 1995. Vol 25:4. P. 853-862.

Ramachandran, V. S., Beuadoin, J. J., Handbook of analytical techniques in concrete science and technology. New York, U.S.A: Noyes Publications/William Andrew Publishing. 990 p. ISBN 0-8155-1437-9

Ramlochan, T. in Course CIV1299S, May 17-21, 2010, University of Toronto, Department of Civil Engineering. 2010.

Scrivener, K. L., Crumbie, A. K., Laugesen, P. The Interfacial Transition Zone (ITZ) Between Cement Paste and Aggregate in Concrete. Interface Science, 2004. Vol 12:4. P. 411-421.

Scrivener, K. L., Damidot, D., Famy, C. Possible mechanisms of expansion of concrete exposed to elevated temperatures during curing (also known as DEF) and implications for avoidance of field problems. Cement, Concrete, and Aggregates, 1999. Vol 21:1. P. 93-101.

SFS-EN 12390-3 Testing hardened concrete. Part 3: Compressive strength of test specimens

SFS-EN 196-3 + A1. Methods of testing cement. Part 3: Determination of setting times and soundness

Soroka, I., Concrete in hot environments. 1st ed. Taylor & Francis e-Library, 2004. 251 p. ISBN 0-203-47363-9

Steefel, C.I. CrunchFlow, Software for Modeling Multicomponent Reactive Flow and Transport. User's Manual. Lawrence Berkeley National Laboratory. 2009

Taylor, H. F. W., Famy, C., Scrivener, K. L. Delayed ettringite formation. Cement and Concrete Research, 2001. Vol 31:5. P. 683-693.

Taylor, H.F.W. Cement Chemistry. 2nd ed. Printed in Great Britain by Redwood Books, Trowbridge, Wiltshire, 1997. 459 p. ISBN 0-7277-2592-0

Thiery, M., Villain, G., Dangla, P., Plaret, G. Investigation of the carbonation front shape on cementitious material: Effect of the chemical kinetics. Cement and Concrete Research, 2007. Vol 37:7. P. 1041-1058.

Thomas, M., Folliard, K., Drimalas, T., Ramlochan, T. Diagnosing delayed ettringite formation in concrete structures, Cement and Concrete Research, 2008. Vol 38:6. P. 841-847.

Tian, H., Xu, T., Wang, F., Patil, V. V., Sun, Y., Yue, G. A numerical study of mineral alteration and self-sealing efficiency of a caprock for CO2 geological storage. ActaGeotechnica, published online 17.7.2013.

Vodák, F.,Trtík, K.,Kapičková, O., Hošková, Š., Demo, P. The effect of temperature on strength-porosity relationship for concrete. Construction and Building Materials, 2004. Vol 18:7. P. 529-534.

Vydra, V., Vodák, F., Kapičková, O., Hošková, Š. Effect of temperature on porosity of concrete for nuclear-safety structures. Cement and Concrete Research, 2001. Vol 31:7. P. 1023-1026.

Wigum, B. J., Pedersen, L. T., Grelk, B., Lindgård, J. State-of-the art report: Key parameters influencing alkali aggregate reaction. SINTEF Building and Infrastructure, 2006. ISBN 82-14-04078-7

www.understanding-cement.com, 28.6.2013

Yang, R., Lawrence, C. D., Lynsdale, C. L., Sharp, H. Delayed ettringite formation in heat-cured Portland cement mortars. Cement and Concrete Research, 1999. Vol 29:1. P. 17-25.

Yang, R., Lawrence, C. D., Sharp, J. H. Delayed ettringite formation in 4-year old cement pastes. Cement and Concrete Research, 1996. Vol 26:11. P. 1649-1659.

Zhang, Z., Olek, J., Diamond, S. Studies on delayed ettringite formation in early-age, heat-cured mortars I. Expansion measurements, changes in dynamic modulus of elasticity, and weight gains. Cement and Concrete Research, 2002. Vol 32:11. P. 1729-1736.

Appendix 1. XRD-diagrams

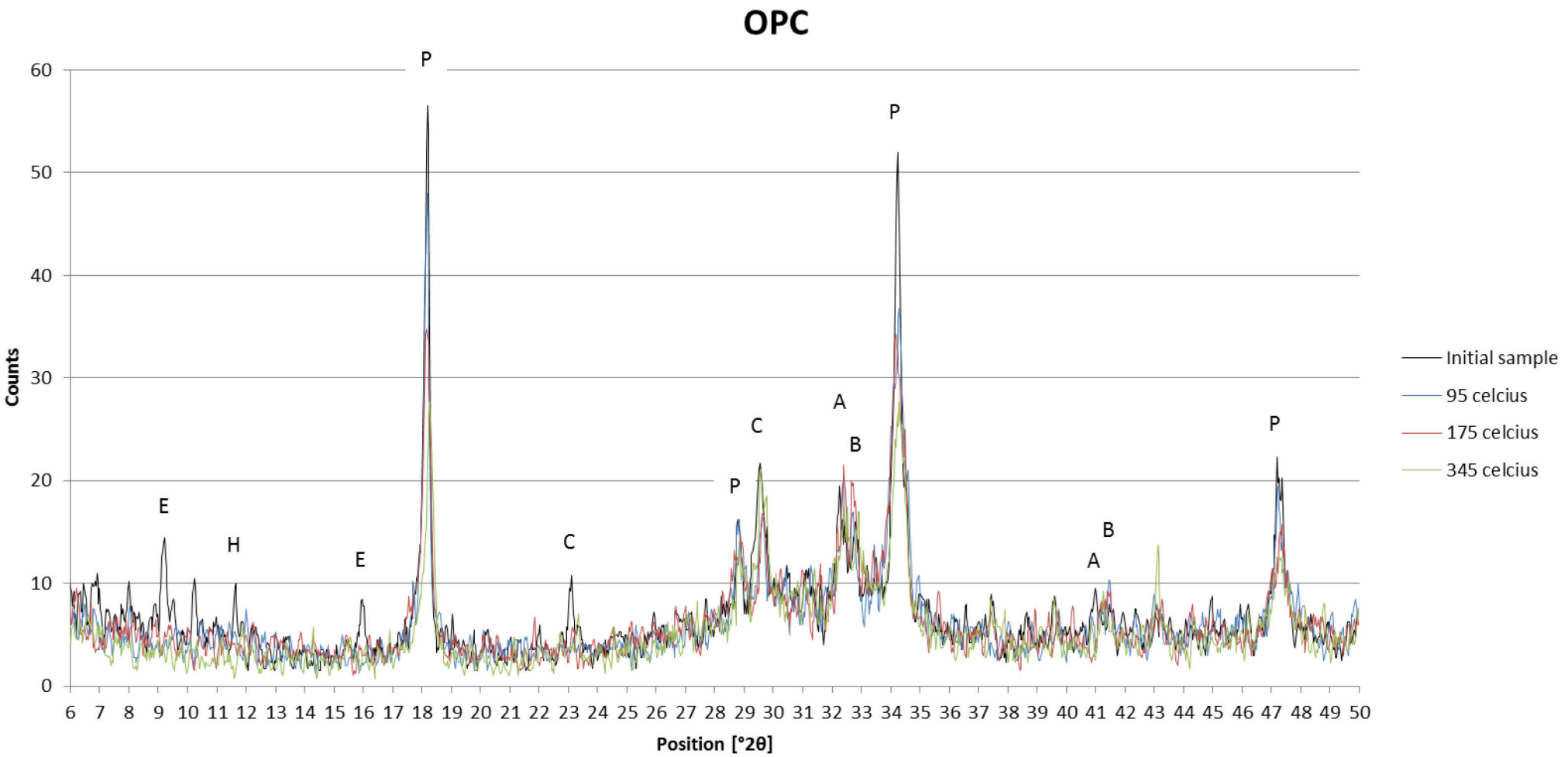
OPC
Counts
Position [°2θ]
Initial sample
95 celcius
175 celcius
345 celcius
P
E
H
C
A
B

, *H*

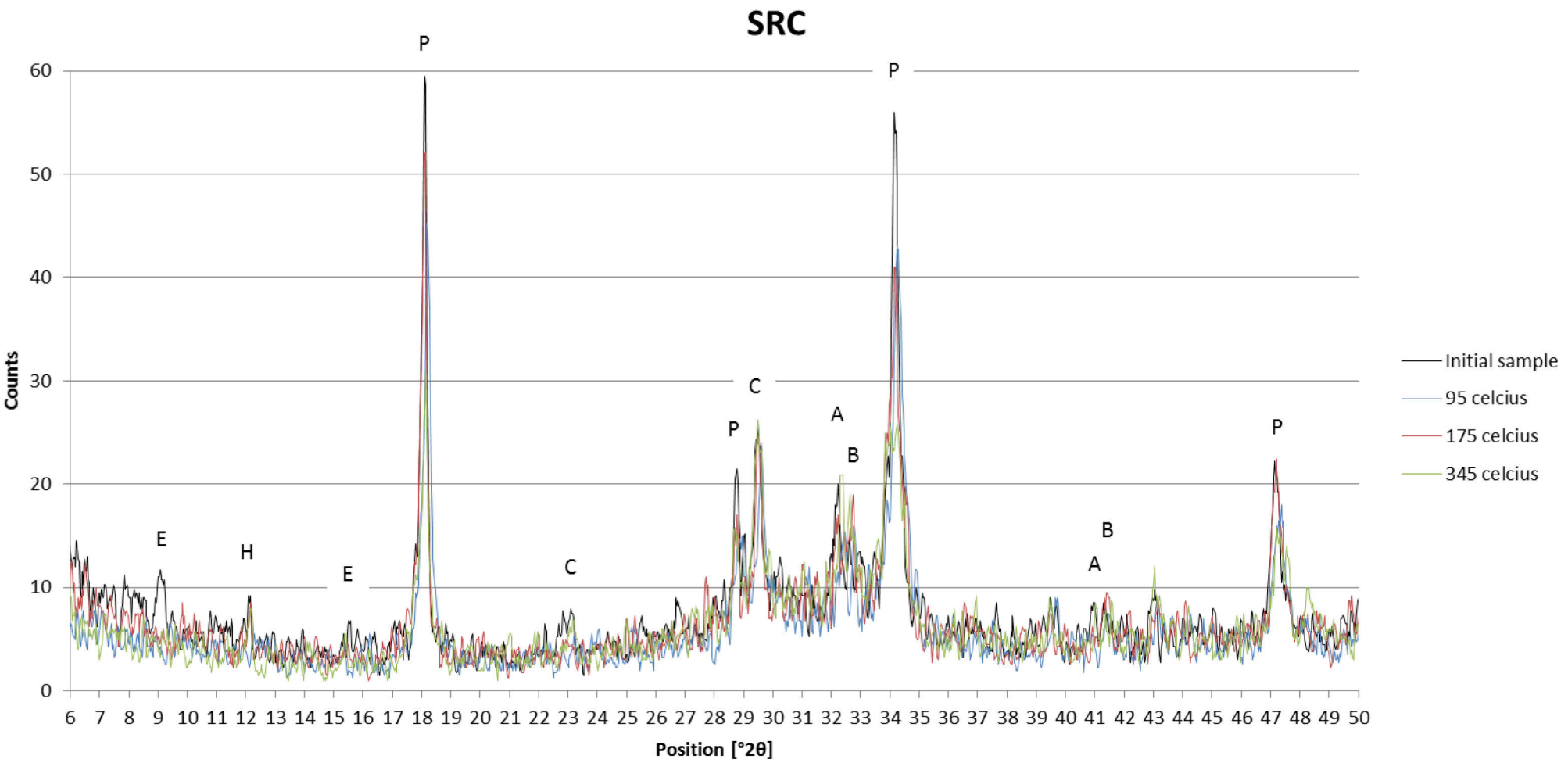
SRC
Counts
Position [°2θ]
Initial sample
95 celcius
175 celcius
345 celcius
P
E
H
C
A
B

lite, H

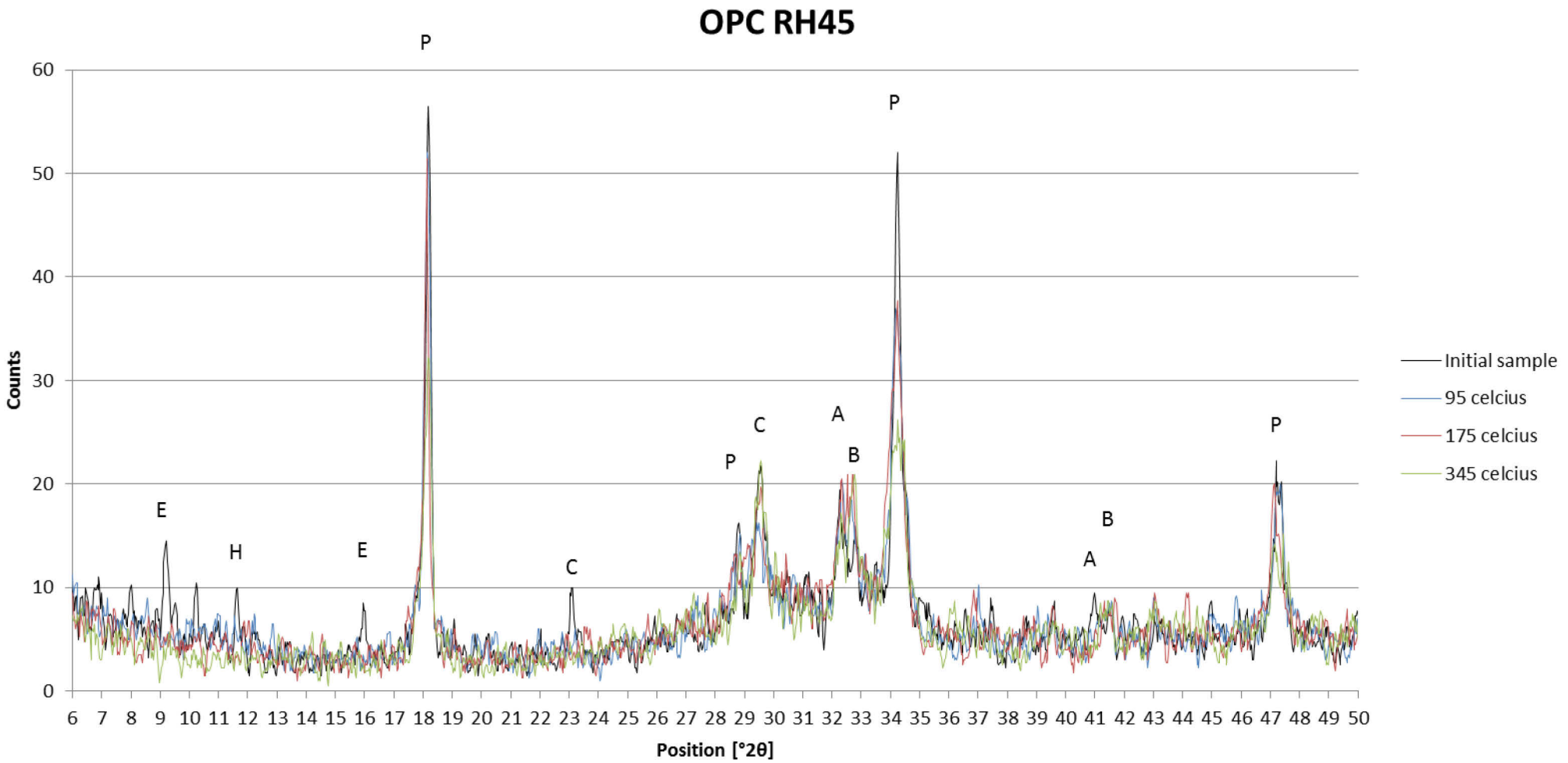
OPC RH45
Counts
Position [°2θ]
Initial sample
95 celcius
175 celcius
345 celcius
P
E
H
C
A
B

alcite, E =

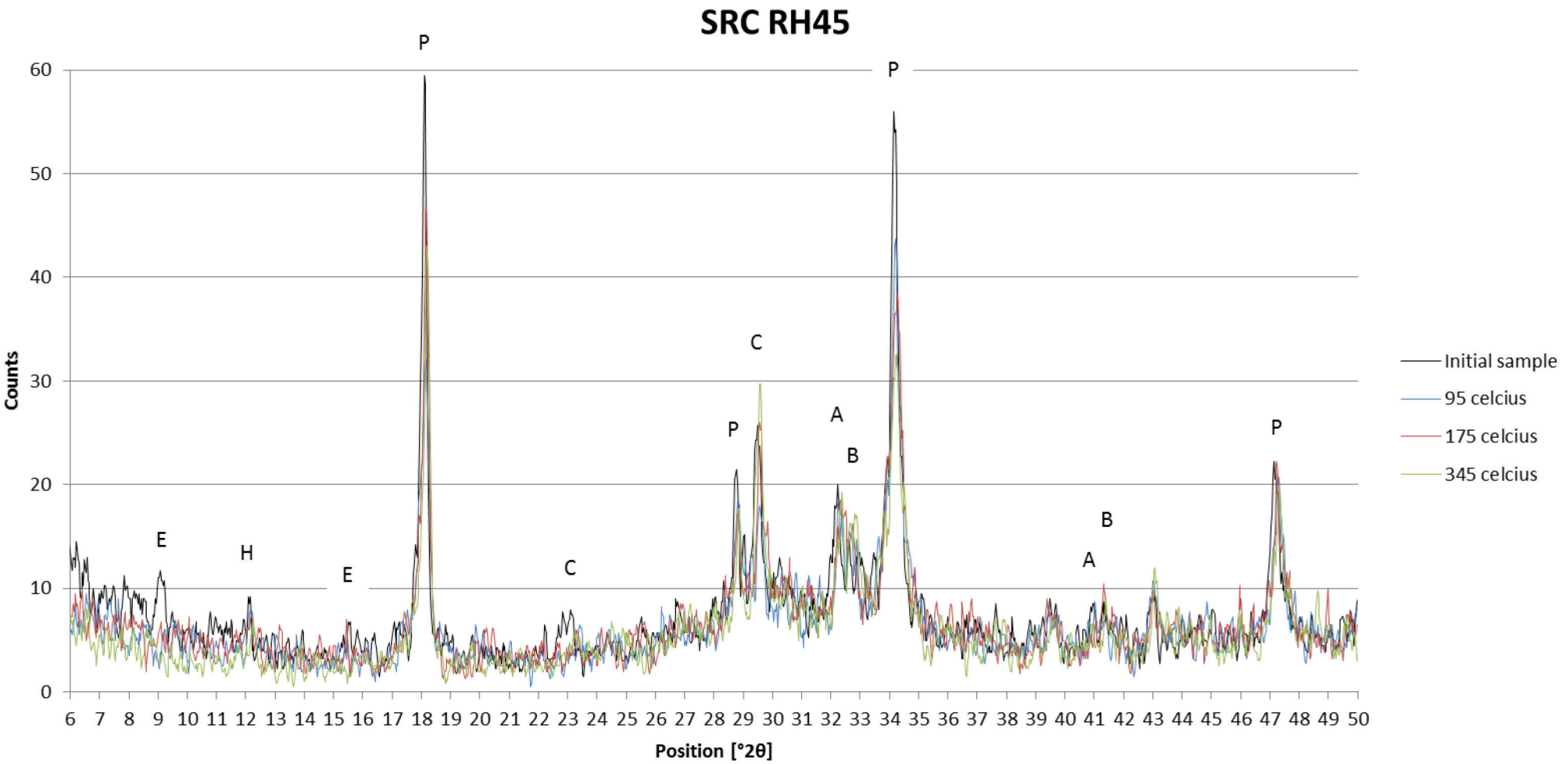
SRC RH45
Counts
Position [°2θ]
Initial sample
95 celcius
175 celcius
345 celcius
P
E
H
C
A
B

calcite,

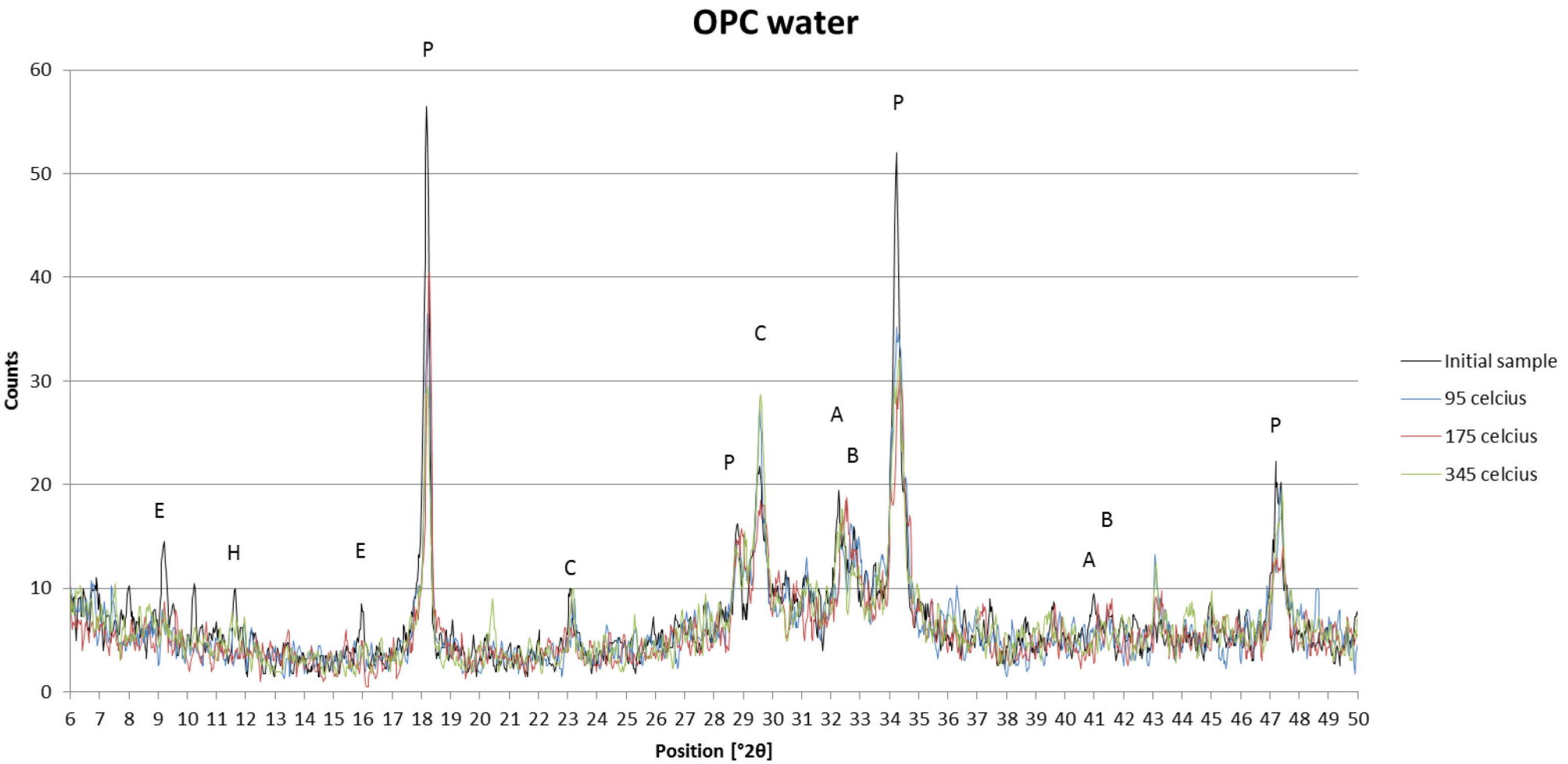
OPC water
Counts
Position [°2θ]
Initial sample
95 celcius
175 celcius
345 celcius
P
E
H
C
A
B

ite, E =

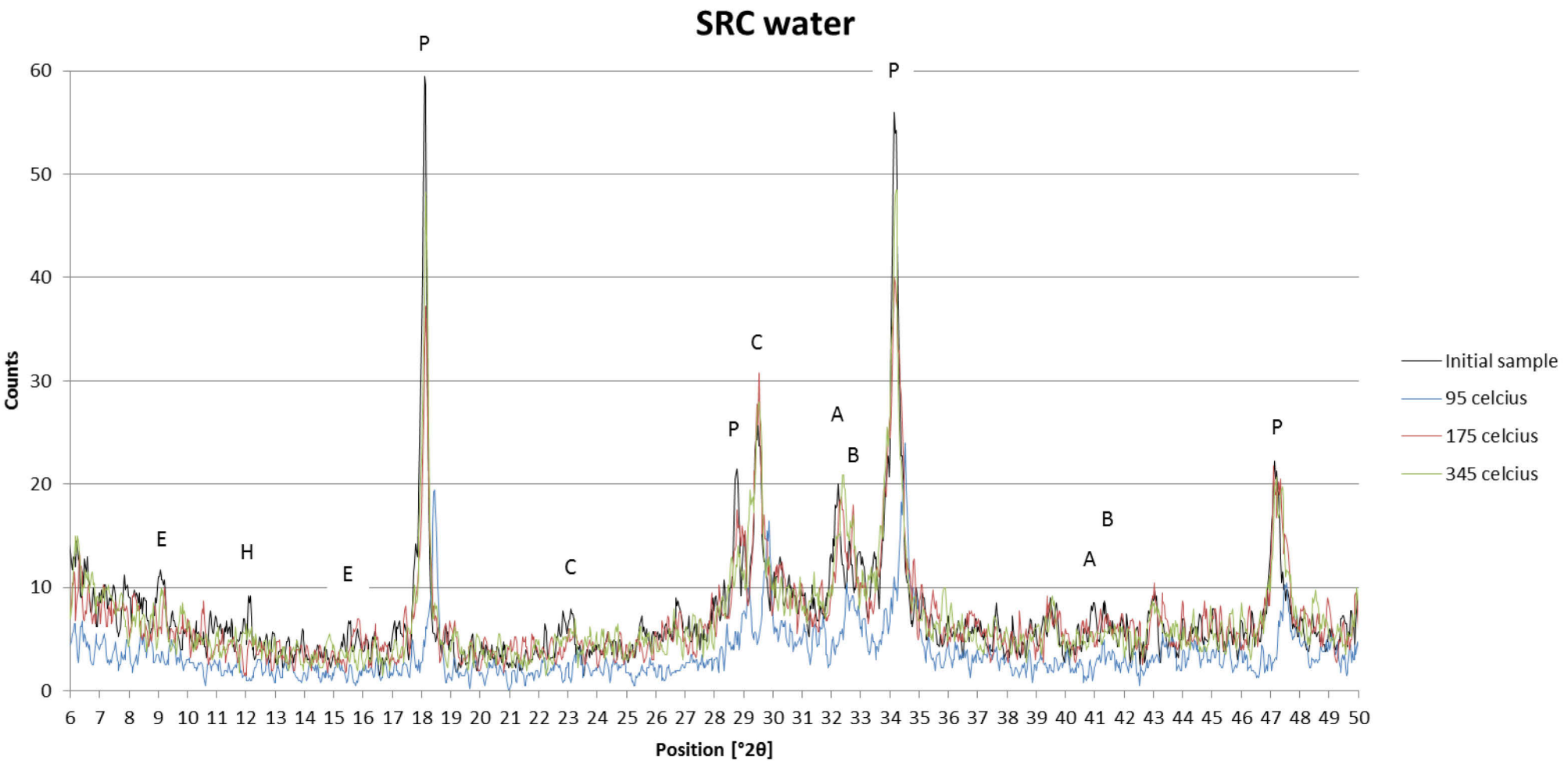
SRC water
Counts
Position [°2θ]
Initial sample
95 celcius
175 celcius
345 celcius
P
E
H
C
A
B

e, E